

Quasi-static and Dynamic Mechanical Analysis of 3D Printed ABS and Carbon Fiber Reinforced ABS Composites

VIGNESHWARAN KARUPAIAH*, VENKATESHWARAN NARAYANAN

Department of Mechanical Engineering, Rajalakshmi Engineering College, Thandalam, Chennai

Abstract: Fused Filament Fabrication (FFF) is the most popular and widely used additive manufacturing process for printing polymer and composite products. Various production factors influenced the strength and stiffness of the part manufactured by 3D printing. A comprehensive experimental analysis was conducted in this study to examine the effect of FFF process parameters (infill density, pattern, and layer thickness) on mechanical properties and their associated failure mechanisms. Tensile, flexural, and impact test specimens were printed using ABS and carbon fibre reinforced ABS filaments in accordance with ASTM standards to investigate the mechanical properties. The results showed that the addition of carbon fiber in ABS increases the mechanical properties. The failure mechanisms are studied using optical microscopy and scanning electron microscopy. Furthermore, dynamic properties are studied over the temperature range from 30°C to 200°C at different frequencies (0.2, 0.5, 1, 2, and 5 Hz) using dynamic mechanical analyzer to investigate the viscoelastic properties (storage modulus, loss modulus, loss factor and glass transition temperature). The results showed that the addition of carbon fiber in the ABS polymer increases the static and dynamic mechanical properties. Moreover, at higher frequencies, the molecular movement in the polymer decreases which in turn stabilizes the composite behavior and reduces the loss factor.

Keywords: Fused Filament Fabrication, ABS, carbon fiber, dynamic mechanical analysis

Additive manufacturing (AM) is the process of building materials layer by layer manner to develop objects as opposed to the traditional manufacturing process. Due to this process capability AM, can fabricate any three-dimensional intricate shaped part, and hence it is preferred over the conventional manufacturing process for producing complex and near net-shaped parts with lesser wastage of material [1]. Some of the important methods of AM are Selective Laser Sintering (SLS), Selective Laser Melting (SLM), Fusion Filament Fabrication (FFF) or Fused Deposition Modeling (FDM), and Stereolithography (SLA). Among several three-dimensional printing (3D) methods. FFF is popular in using polymer filaments because of its simplicity, ease of handling, and potential applicability of the method [2]. With the development of AM Technology, now revolutionizes both design and manufacturing which enables it to be a part of industrial revolution 4.0 in various sectors such as aerospace, energy, automotive, medical, tooling, and consumer goods [3]. This revolution results in virtual data merging with real production equipment [4]. A key component in making Industry 4.0 is that the machine can produce the component faster, more flexible, and more precise than ever before. It will have to be possible to return data into components and products at incredible speed. Although, additive manufacturing is growing popular day by day and it is hoped that in the future it will be a home gadget to make food, toys, etc. [5]. Dey et al. [6] summarized the optimization of FFF process parameters and their influence on tensile and flexural properties. The results proved that the quality of printed parts through the FFF process can be improved by optimizing the process parameters such as infill density, infill pattern, layer thickness, raster angle, and part build orientation. Fernandez et al. [7] studied the effect of infill density (20%, 50%, and 100%) and pattern (Rectilinear, Honeycomb, and Line) on the tensile strength of Acrylonitrile Butadiene Styrene (ABS) material using the FFF technique. They have concluded that the rectilinear pattern with 100% infill density has higher tensile strength than the honeycomb pattern due to its better deposition trajectory bonding between previous layers. Ning et al. [8] analyzed the tensile properties of ABS and Carbon fiber reinforced ABS in fused deposition modeling by varying 3, 5, 7.5, 10 and 15 wt. % of carbon. The result established that by adding carbon fiber with 5 wt. % had better tensile strength while better young's

*email: venkateshwaran.n@rajalakshmi.in

modulus is achieved in 7.5wt. %. Further, with the addition of 10 wt.% of carbon fiber, the tensile strength decreases due to the presence of porosity in the specimen when analyzed using micrographic images. Dave et al. [9] evaluated the tensile properties of Polylactic acid (PLA) by varying infill pattern, infill density, and part orientation. The results revealed that higher tensile strength was obtained when specimens were built with flat and long edge part orientation as compared to on short edge orientation with the rectilinear and concentric patterns. Bogrekei et al. [10] studied the effect of infill pattern and density on the hardness property of fusion deposition modeling PLA printed material. The result showed that the specimen with a hexagonal pattern had the maximum hardness for all infill densities due to its better deposition trajectory and interlayer bonding. Jatti et al. [11] analyzed the influence of FFF process parameters (Layer thickness, infill density, and printing speed) on the mechanical properties of PLA filament material. It has been observed that infill density has a maximum effect on tensile strength and flexural strength because more infill percentages indicate more material is been deposited into the fabricated part and hence the density of the part increases. Thus, more strength is required to pull and break the specimen. Shubham et al. [12] studied the influence of layer thickness (0.075, 0.10, 0.25, and 0.50 mm) on mechanical properties of 3D printed ABS polymer by the FFF process. The study demonstrated that mechanical properties decrease, with an increase in layer thickness because the specimens prepared with a lesser layer thickness (0.075 mm) are closely stacked together and provide a better bond between the layers. Nugroho et al. [13] evaluated the effect of layer thickness on flexural properties of PLA and observed that with 0.5 mm layer thickness there were significant increases in flexural strength and stiffness.

Kumar et al. [14] summarized the effects of mechanical properties and microstructure of 3D printed polycarbonate reinforced ABS composite materials. It was observed that the flexural strength of the 3D printed PC/ABS is relatively higher than compression molding PC/ABS at 30 wt. % polycarbonate. Vigneshwaran et al. [15] evaluated the mechanical properties of wood-PLA composite printed using FFF process with different infill density (30, 60 and 90%), infill pattern (layer, triangle, and hexagon), and layer thickness (0.08, 0.16, and 0.24 mm). The result showed better properties were achieved with an increase in infill percentage. Also, the properties such as toughness and energy absorption rate are increased with an increase in infill density in the honeycomb pattern. Christiyan et al. [16] studied the influence of process parameters such as layer thickness (0.2, 0.25, and 0.3 mm) and Printing speed (30, 40, and 50 mm/s) on the mechanical properties of 3D printed hydrogen magnesium silicate reinforced ABS composite. The results revealed that a low printing speed of 30 mm/s and 0.25 mm layer thickness gives better tensile and flexural properties due to better bonding between the layers at low printing speed with lesser layer height. Wenzheng et al. [17] analyzed the influence of layer thickness (200 μ m, 300 μ m, 400 μ m) and raster angle (0°, 35°, and 40°) on the mechanical properties of 3D printed Poly Ethyl Ether Ketone (PEEK) and ABS material. The results summarized that the optimal tensile properties of PEEK printed samples were higher than ABS at 300 μ m layer thickness and 0° raster angle. Tekinalp et al. [18] evaluated the tensile properties of ABS and carbon fiber reinforced ABS composites by varying the carbon weight percent as 10, 20, 30, and 40. The tensile strength and modulus of printed samples showed an increase of 115% and 700%, respectively in the compression molding process. Anderson [19] studied the mechanical properties of the virgin and recycled polylactic acid by the FFF process and the result showed that the recycled filament degrades due to extrusion interruptions and limited interlayer adhesion which leads to defects in the specimen and progressively decreases the mechanical properties. Papon et al. [20] evaluated the tensile properties and fracture behavior of 3D printed carbon nano fiber-reinforced composites. The results revealed that superior tensile modulus and strength for the same strain rate observed in 0.5% CNF/PLA composites compared to the neat PLA matrix due to proper bonding between CNF and PLA and low agglomeration. Akhoundi et al. [21] studied the tensile properties of continuous fiber-reinforced thermoplastic composites produced by the FFF process revealing that the high fiber to matrix volume content yields high mechanical strength. Also, the rectangular type laying pattern eliminates the misalignment of fiber with the loading axis.

From the above-listed literature the following conclusions can be drawn:

FFF process is widely used to prepare polymer and polymer composite parts because of the flexibility it offers. Further, it is noted that the process parameters play an important role in developing products with good

strength, quality, and surface roughness and therefore, the identification of crucial and optimum process parameters is very essential for better improvement in the quality of parts printed by FFF. To the best knowledge of the authors, limited studies are available on static and dynamic mechanical properties of carbon/ABS composite. Hence, in this novel work, the influence of process parameters: layer thickness, infill pattern, and infill density on static and dynamic mechanical characteristics of ABS and carbon fiber reinforced ABS composite was investigated. Further, the fractured surfaces of tested specimens were investigated using optical microscopy and scanning electron microscopy.

2. Materials and methods

2.1. Materials

The materials used in this study were Acrylonitrile Butadiene Styrene (ABS) and Carbon fiber reinforced Acrylonitrile Butadiene Styrene (CF-ABS) filaments, as shown in Figure 1. They are obtained from NANOVIASmart Chemicals, France, and their properties are given in Table 1. ABS is a thermoplastic material that is light in weight, abrasion-resistant, and has good impact properties. The carbon fiber population is 5% of the mass fraction in the CF-ABS filament. The filament diameter of 1.75mm was used to fabricate the specimens as per the ASTM standard using the FFF techniques. The filament diameter was verified using optical microscopy, as shown in Figure 2. Table 2 shows the printing parameter used in this work.



Figure 1. ABS and CF-ABS filaments



Figure 2. Optical micrographs of CF-ABS filament

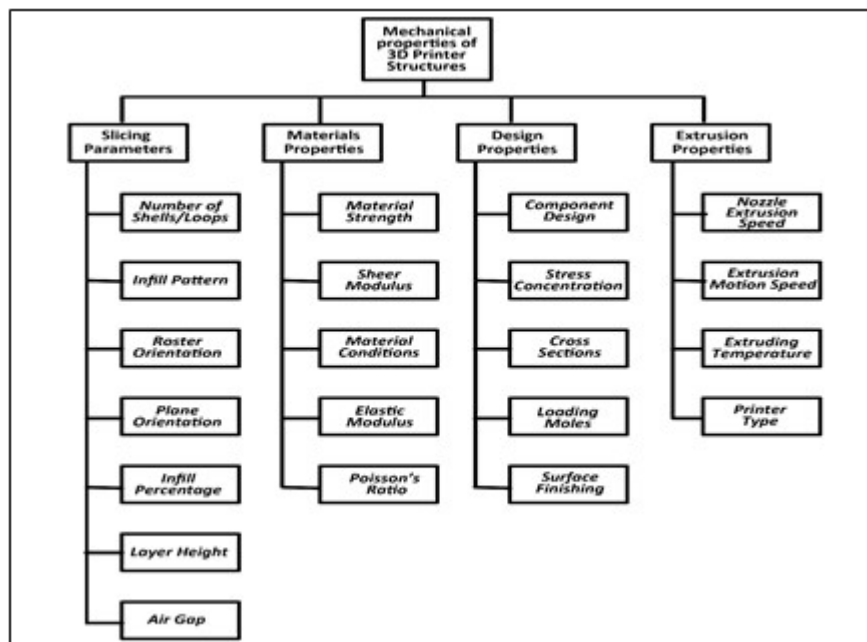
Table 1. Physical and mechanical properties of filament (As per manufacturer data)

Filament	Colour	Density (g/cm ³)	Tensile Strength (MPa)	Tensile Modulus (GPa)	Flexural Strength (MPa)	Flexural Modulus (GPa)
ABS	White	1.04	40	2.1	50	2.5
ABS-CF	Deep Black	1.08	42	2.7	70	2.7

Table 2. Printing parameters

Parameters	Values
Nozzle Diameter	0.4 mm
Nozzle Temperature	240°C
Bed Temperature	90°C
Orientation	Flat Orientation
Raster Angle	0°
Contours	2 shell

The mechanical properties of 3D printed parts depends on factors such as material properties, slicing parameters, extrusion parameters, design properties, etc. which are depicted as a flow chart diagram, as shown in Figure 3. This diagram represents a series of independent events or conditional probabilities. In this study, the infill density, infill pattern, and layer thickness are varied experimentally and the samples are prepared through the FFF process. The microscopic image of three different infill patterns (Grid, Hexagon, and Rectilinear) of the fabricated specimens are visualized using an optical microscope and is as shown in Figure 4.

**Figure 3.** Flow chart for process parameters**Figure 4.** Optical microscopic image of infill pattern

There are a variety of parameters that play a dominant role in the mechanical strength of a material. As per the flowchart diagram and full factorial statistical design shown in Table 3, the major parameters such as infill density, infill pattern, and layer thickness are varied, and specimens were prepared accordingly. Using ABS and CF-ABS composite filament a large number of samples are printed to evaluate their mechanical properties. A matrix data is constructed and shown in Table 4 for the printed specimen. The matrix table indicates G1, G2, G3, G4, G5, G6, G7, G8, G9, H1, H2, H3, H4, H5, H6, H7, H8, H9 and R1, R2, R3, R4, R5, R6, R7, R8, R9 designated for the samples with a grid, hexagon, and rectilinear pattern with different infill percentage and layer height respectively. For pure ABS printed specimens G, H, and R have been designated with capital letters while the CF-ABS composite printed samples are designated with small letters g, h, and r.

Table 3. Process parameter level and value

Process Parameter	Level 1	Level 2	Level 3
Layer height	0.15 mm	0.20 mm	0.30 mm
Infill pattern	Grid	Hexagonal	Rectilinear
Infill density	0%	25%	50%

Table 4. Process parameter combination and its designation

Layer Height (mm)	Infill Density (%)	Infill Pattern		
		Grid	Hexagon	Rectilinear
0.15	0	G1	H1	R1
	25	G2	H2	R2
	50	G3	H3	R3
0.20	0	G4	H4	R4
	25	G5	H5	R5
	50	G6	H6	R6
0.30	0	G7	H7	R7
	25	G8	H8	R8
	50	G9	H9	R9

2.2. Specimen printing

As per the process parameter combinations listed in Table 4, the specimens were printed for experimental testing as per ASTM standards. The printed specimens were subjected to perform the tests to determine the mechanical properties. Figure 5 shows the printed samples and experimental setup of this work.

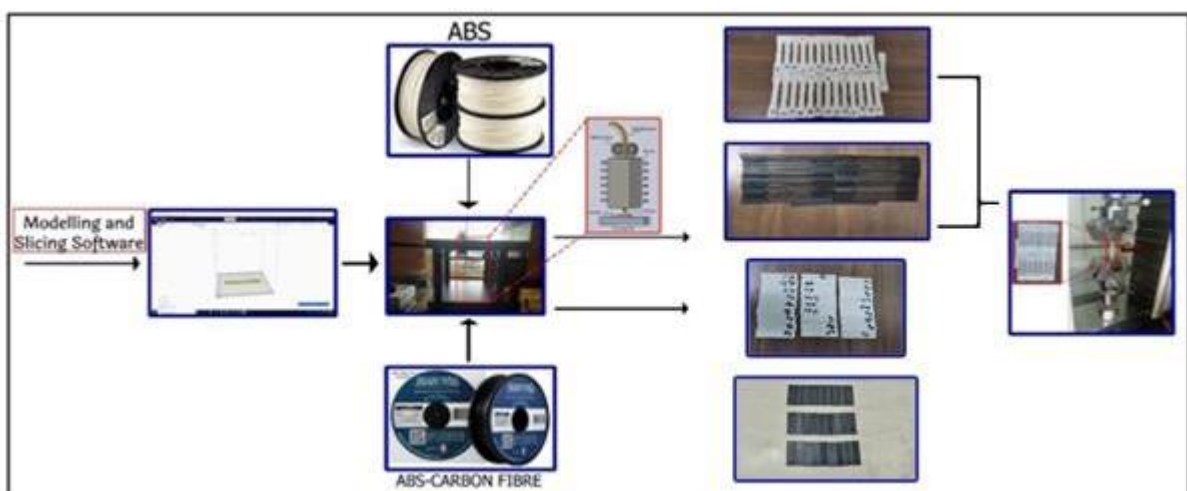


Figure 5. FFF printing process

2.3. Testing methods

2.3.1. Mechanical properties

The specimens are printed according to ASTM D638 [22] for the tensile test, ASTM D790 [23] for three-point bending test, and ASTM D256 [24] for the Izod impact test. Tensile and flexural tests were performed using a computerized universal testing machine (Instron Series- 3382 model) at a crosshead speed of 2 mm/min and 1.3-1.5 mm/min, respectively.

2.3.2. Dynamic analysis

Using Dynamic Mechanical Analyzer (Model: SEIKODMAI-DMSC 6100), the influence of temperature and frequency on the modulus and damping characteristics were evaluated as per ASTM D7028, having the dimension of 40mm × 13mm × 3mm used. The specimens were tested under tensile mode with a temperature range from 30°C to 200°C at different frequencies (0.2, 0.5, 1, 2 and 5 Hz) and a heating rate of 5°C/min.

2.3.3. SEM analysis

The failure mechanisms of the specimens were investigated using Hitachi S3400N scanning electron microscopy with an accelerating voltage of 15kV. The SEM images are used to visualize the bonding between the layer printed using the FFF process and also to determine the distribution and interactions of the carbon fiber in the ABS polymer matrix.

3. Results and discussions

3.1. Tensile properties of ABS printed specimen

As per the matrix data for specimen combinations shown in Table 4, different ABS specimens were prepared through the fusion filament fabrication by varying the infill density, pattern, and layer height. Figures 6 and 7 show the tensile strength and modulus of ABS printed samples. The result is plotted as a variety of process parameters: layer height, infill density, and infill pattern on tensile strength and modulus, respectively. From the analysis, specimen H9 which is the combination of (Hexagonal pattern, 0.30 mm layer height, and 50 % infill density) showed a better tensile strength of 17.13 MPa and tensile modulus of 1.50 GPa. From the results, it was observed that the infill density is proportional to the mechanical properties. As the infill density increases progressively, the tensile strength and modulus also increase. This is due to the reason that a higher level of infill density results in a lower amount of void in the infill pattern, and subsequently increases the strength and modulus. This situation is similar to three different types of infill patterns [7]. The hexagonal infill pattern specimen shows increased tensile strength and modulus as compared to the grid and rectilinear pattern due to the honeycomb structure. The honeycomb structure is strong, carries a large load, and does not buckle easily when bent. It can be seen that the bonding zone between each layer is different in each pattern. In the hexagonal pattern, each layer lays down on a similar previous layer. While in rectilinear and grid patterns, the bonding zone between each layer corresponds only with the points where the filament crosses the previous layer filaments. These characteristics revealed a reason for achieving better tensile strength and modulus in the hexagonal pattern printed samples which are shown in Figure 8 [7-10].

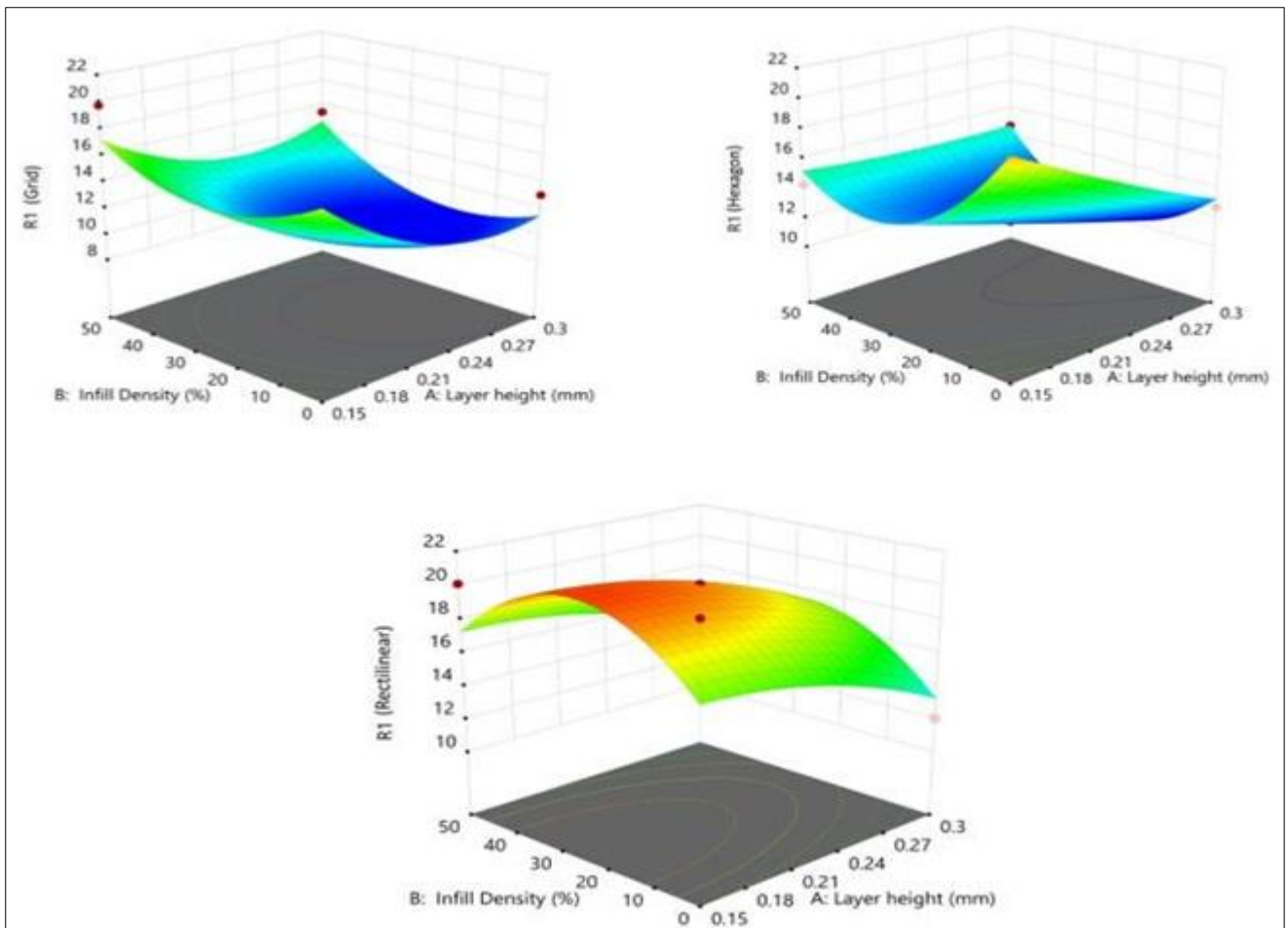


Figure 6. Surface graph prediction for Tensile strength of ABS specimens

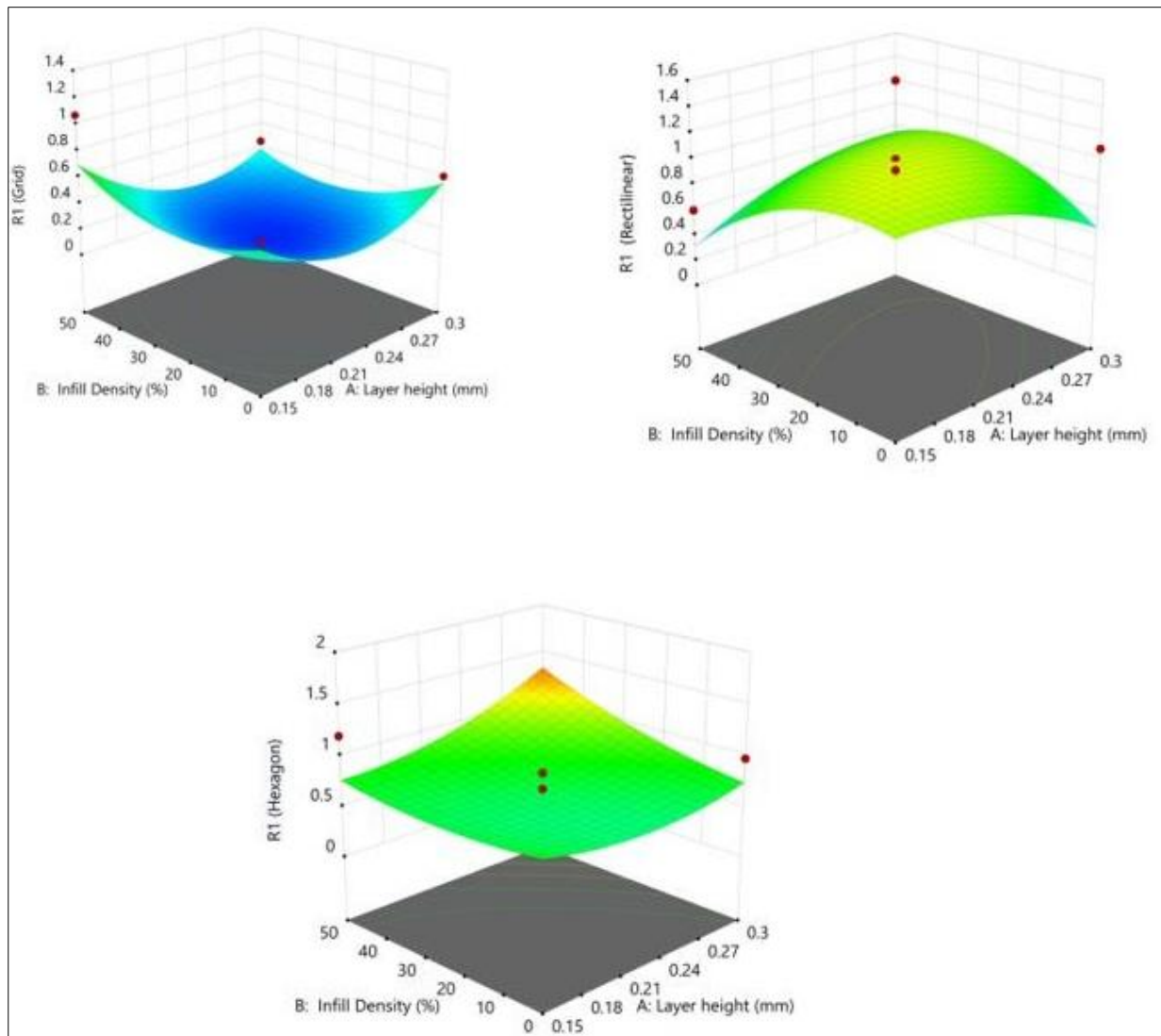


Figure 7. Surface graph prediction for tensile modulus of ABS specimens

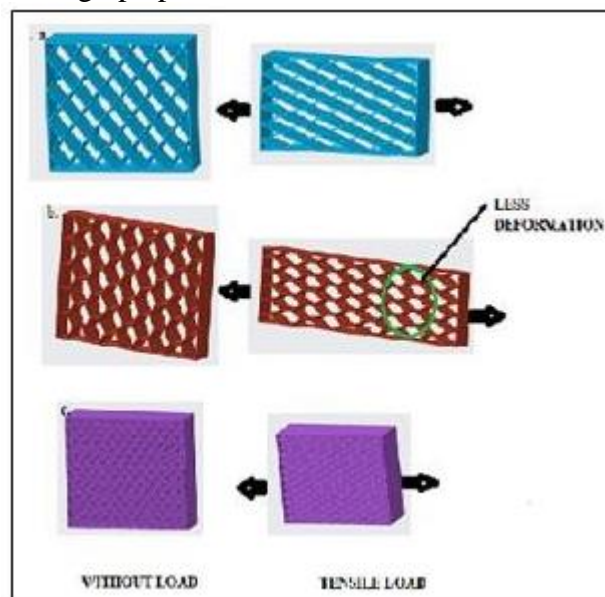


Figure 8. a. Strength mechanism in a grid pattern; b. Strength mechanism in hexagon pattern; c. Strength mechanism in a rectilinear pattern

3.2. Tensile properties of CF-ABS printed specimen

Figures 9 and 10 show the tensile strength and modulus of the composite specimens, respectively. From the analysis, specimen h9 combination of (Hexagonal pattern/0.30mm layer height/50% Infill density) shows the optimal tensile strength of 21.41MPa and better tensile modulus of 1.47 GPa. When comparing with the results of the ABS specimens, the results of the composite specimen showed that an increment in tensile properties and it is achieved due to the incorporation of stiffer carbon fiber in the ABS matrix. Hence, the reason for optimal properties is very similar to that explained by pure ABS printed specimens. Similarly, on observing the tensile modulus of CF-ABS printed samples, their values increased with an increase in infill density from 0% to 25%, but there is a small decrease in value in 50% infill density. This difference may be occurred due to the presence of infill fibers in the polymer matrix which deform and absorb the load. This capability increases as the infill density increases. When that density starts to create bonds between the different sections of the pattern, the tensile strength improves. However, the increase in the ability to deform is reduced [11, 12].

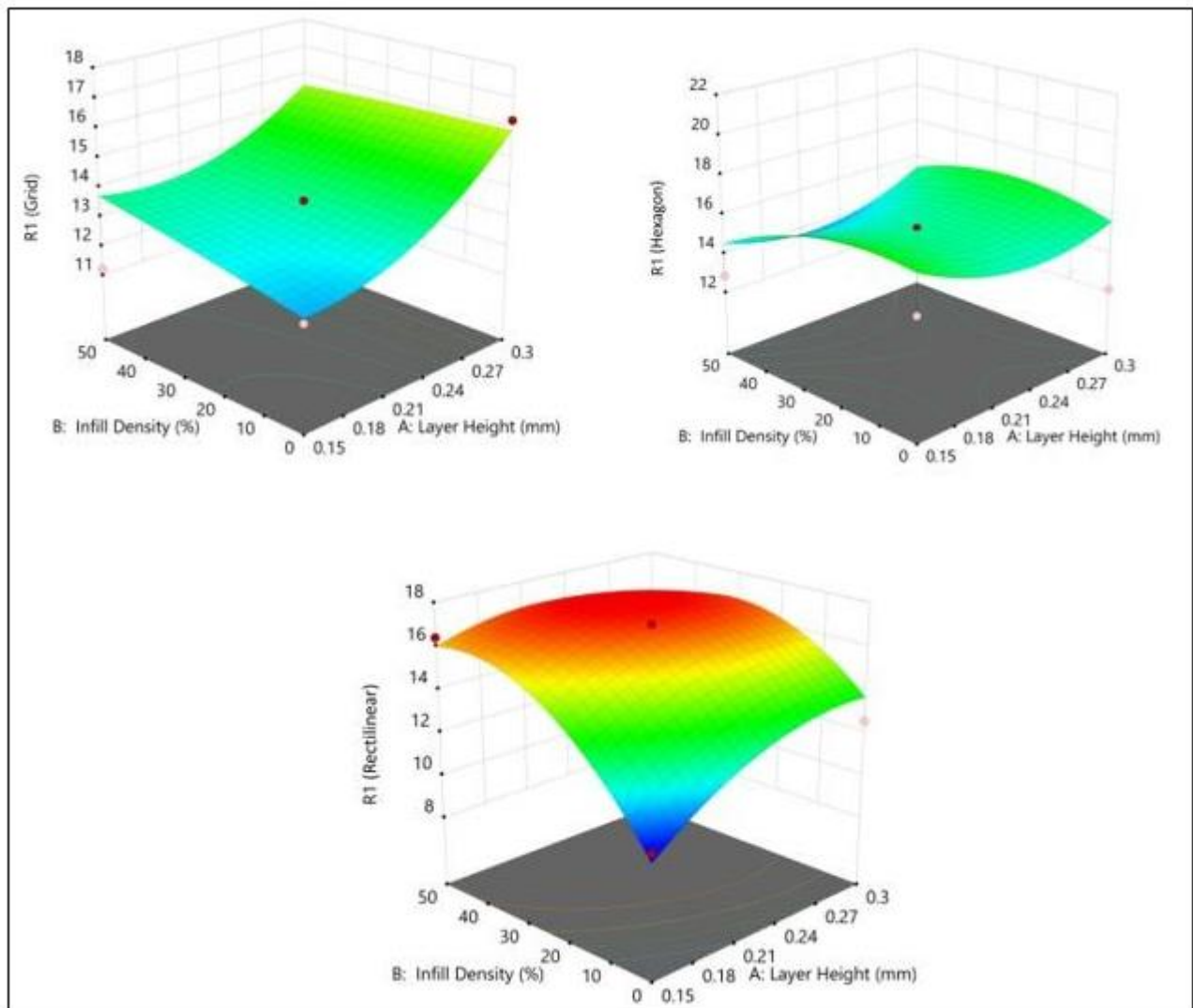


Figure 9. Surface graph prediction for tensile strength of CF-ABS specimens

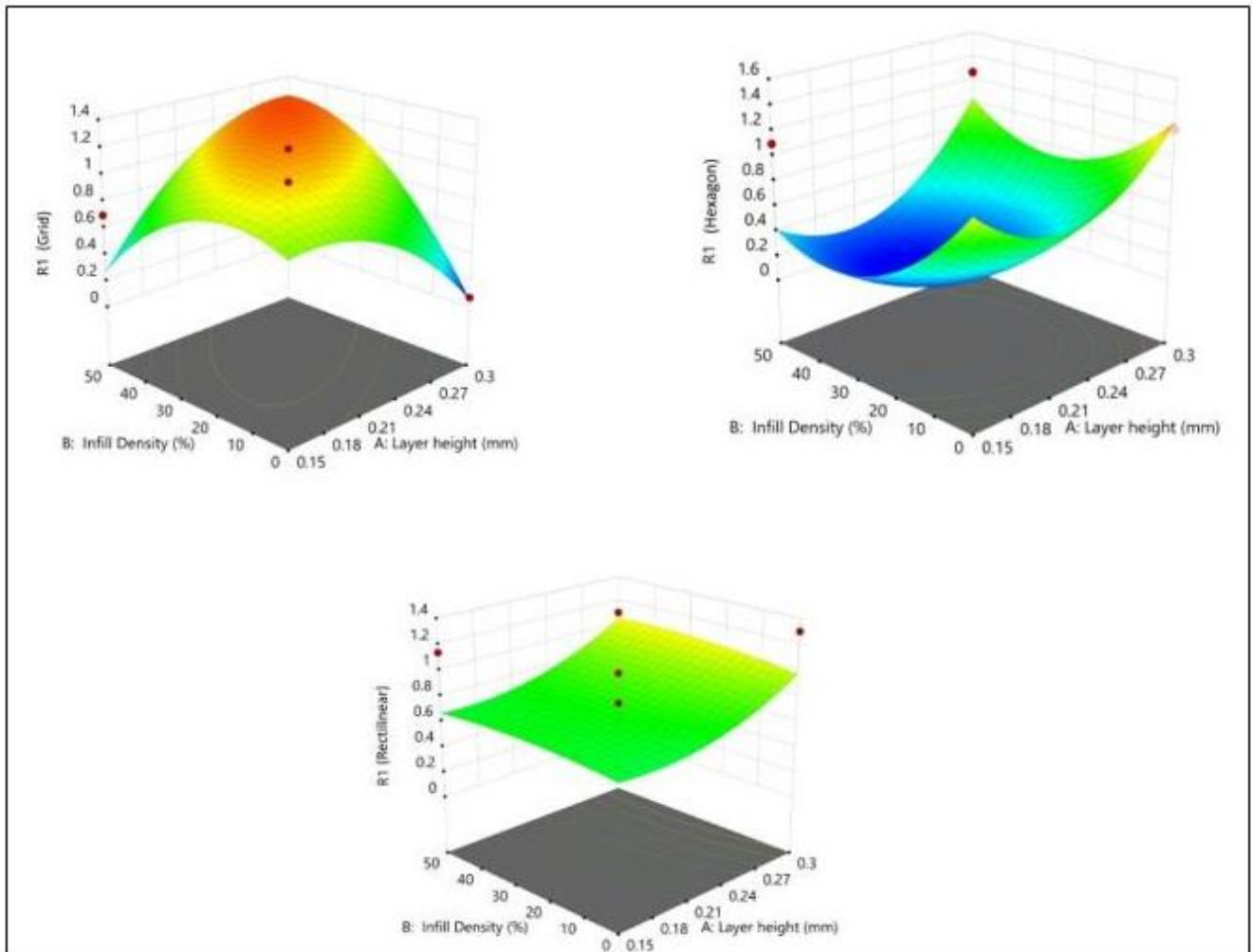
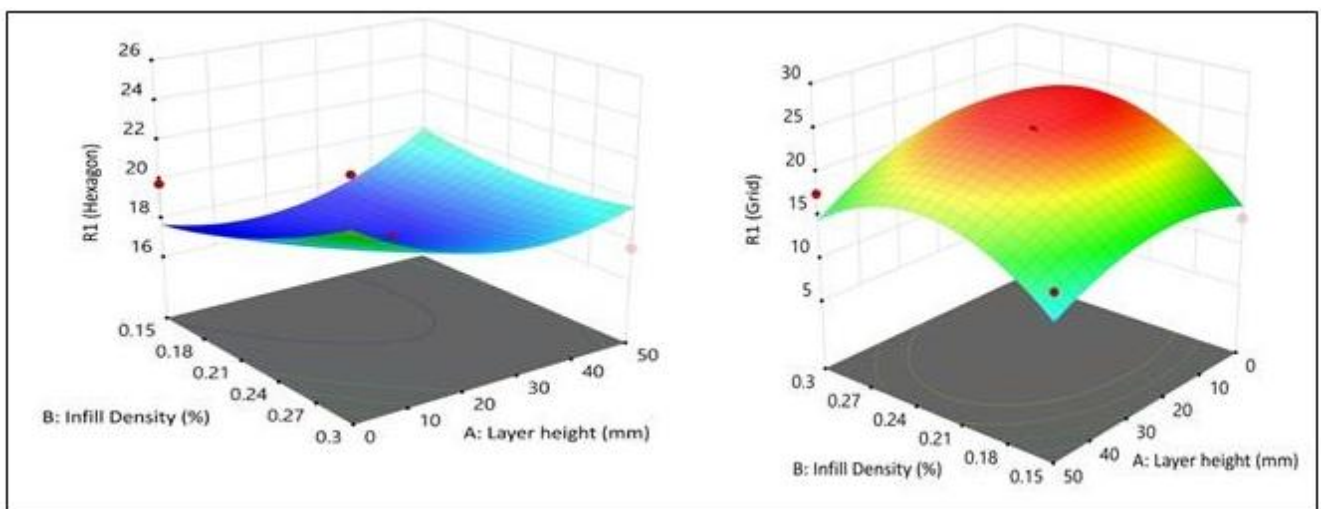


Figure 10. Surface graph prediction for tensile modulus of CF-ABS specimens

3.3. Flexural properties of ABS printed specimen

Similar to tensile specimens, different ABS printed flexural specimens are prepared as per the matrix data combinations shown in Table 4. Figures 11 and 12 represent the flexural strength and modulus of ABS printed specimens, respectively. Using the design of experiment software, the data is plotted as a variety of process parameters on flexural strength and modulus.



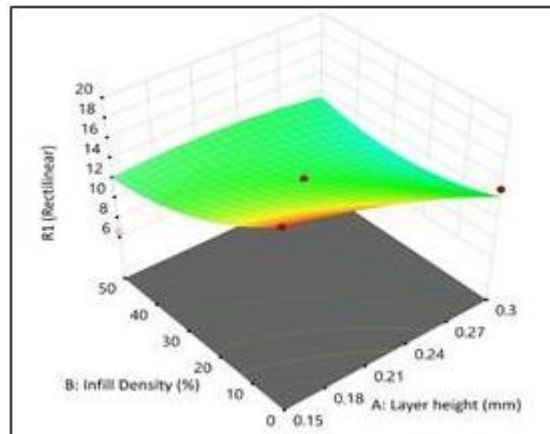


Figure 11. Surface graph prediction for flexural strength of ABS specimen

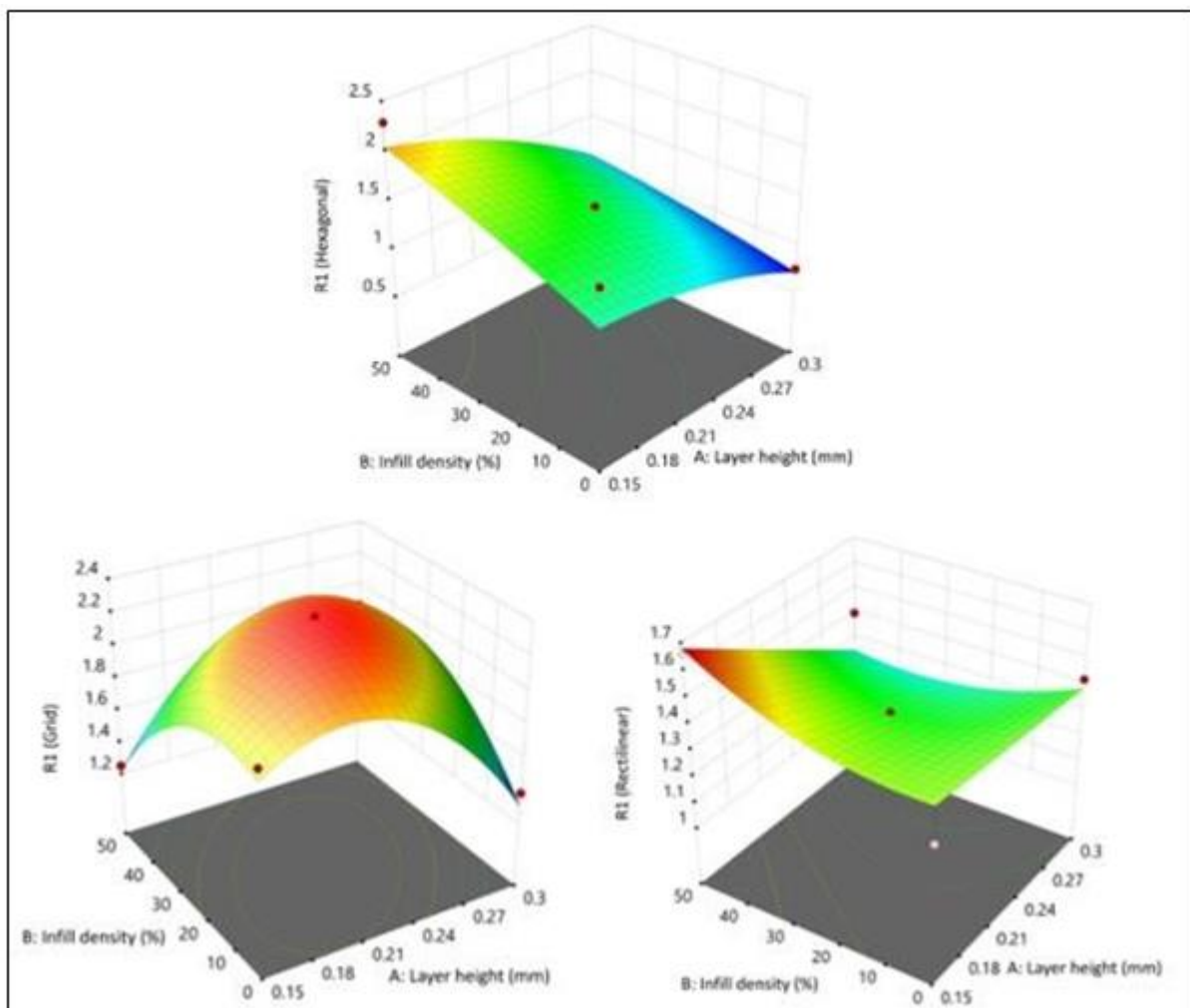


Figure 12. Surface graph prediction for flexural modulus of ABS specimen

3.4. Flexural properties of CF-ABS printed specimen

The flexural properties of CF-ABS composite are shown in Figures 13 and 14. From these figures, it is observed that mechanical properties are strongly dependent on layer height, infill density, and infill pattern. The specimen printed with a combination of (Hexagonal pattern / 0.30mm layer height / 50% Infill density)

shows the optimal flexural strength of 24.2 MPa and modulus of 1.43 GPa. Secondly, the effects of the addition of carbon fiber in the ABS matrix were analyzed. When comparing to the pure fiber in the ABS polymer, the increase in maximum flexural strength and modulus were attained in the same combination as listed for the tensile properties. These results can be attributed to the remarkable strength and modulus of carbon fiber reinforcement given that the mechanical performance of composites normally can be enhanced via the incorporation of superior reinforcement with a higher stiffness than the matrix. Overall, the flexural properties are increased by 20 to 25 % when compared to pure ABS. As the infill density increase from 0 to 50 %, the flexural strength and modulus increase. On the other hand, the changes in the infill pattern type directly change the internal structure of the sample, thereby affecting its flexural strength. Based on the graph, the result shows an inconsistent value for the layer thickness of 0.20 to 0.30 mm. This problem could happen due to an unforeseen error during experimentation such as temperature and humidity conditions. When the layer height increases from 0.20 mm to 0.30 mm, at 0.30 mm fragile interlayer bonding causes a reduction in bending strength and triggered the delamination of welded layers. An increase in layer height results in shrinkage defect on the top of the previous layer [13]. The results revealed that tensile and flexural properties were increased due to the addition of carbon fiber in the polymer composites. Due to the excellent properties of carbon fiber, the composite properties were increased when compared to the properties of ABS specimens. A similar research study proves that carbon fiber content first increases the mechanical properties from 0 wt.% to 5 wt.% and then it decreases from 5 wt.% to 10 wt.%. Porosity is the main reason for their decrement in strength with the addition of 10 wt.% carbon content in the ABS polymer. This phenomenon could be the reason for adding carbon fiber content up to 5 wt.% and further addition resulted in the smallest value of tensile and flexural properties [14-17].

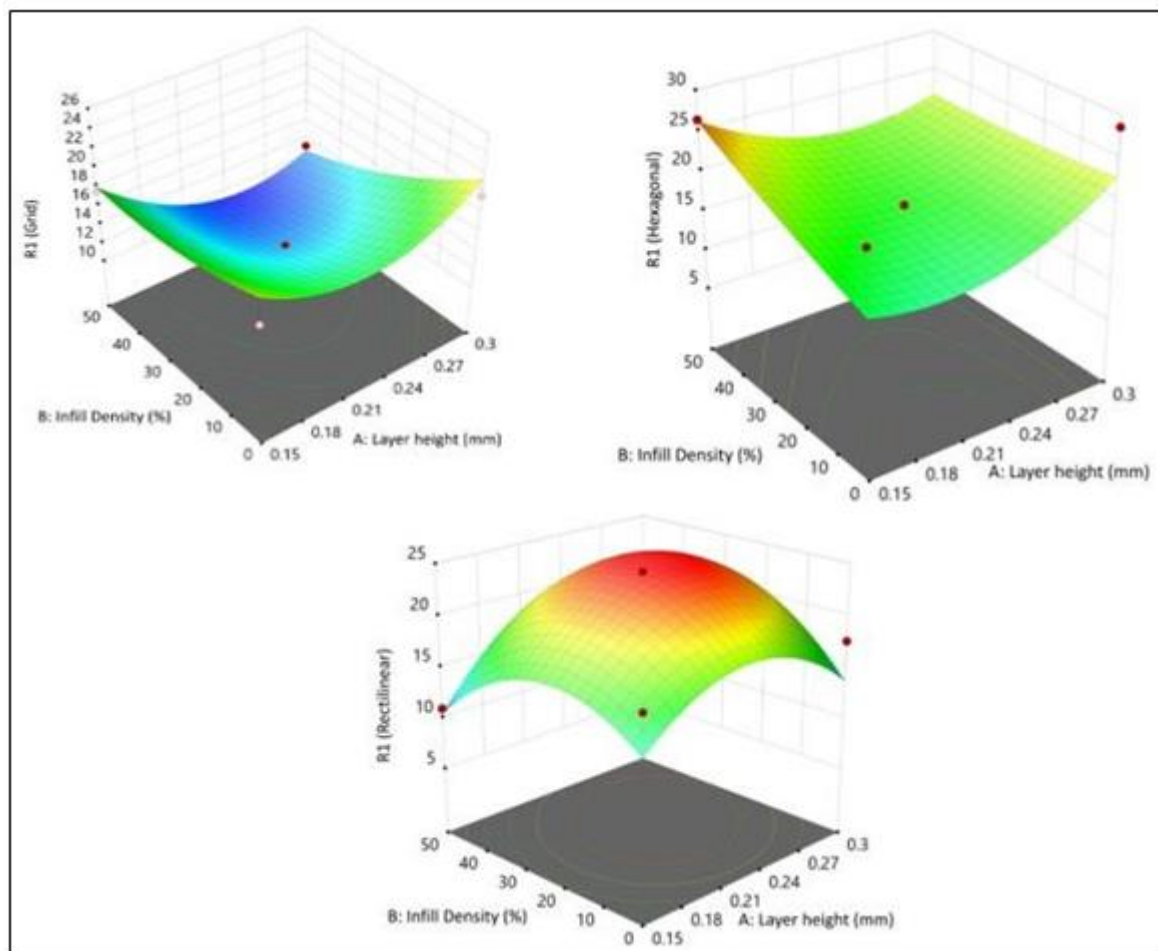


Figure 13. Surface graph prediction for flexural strength of CF-ABS specimen

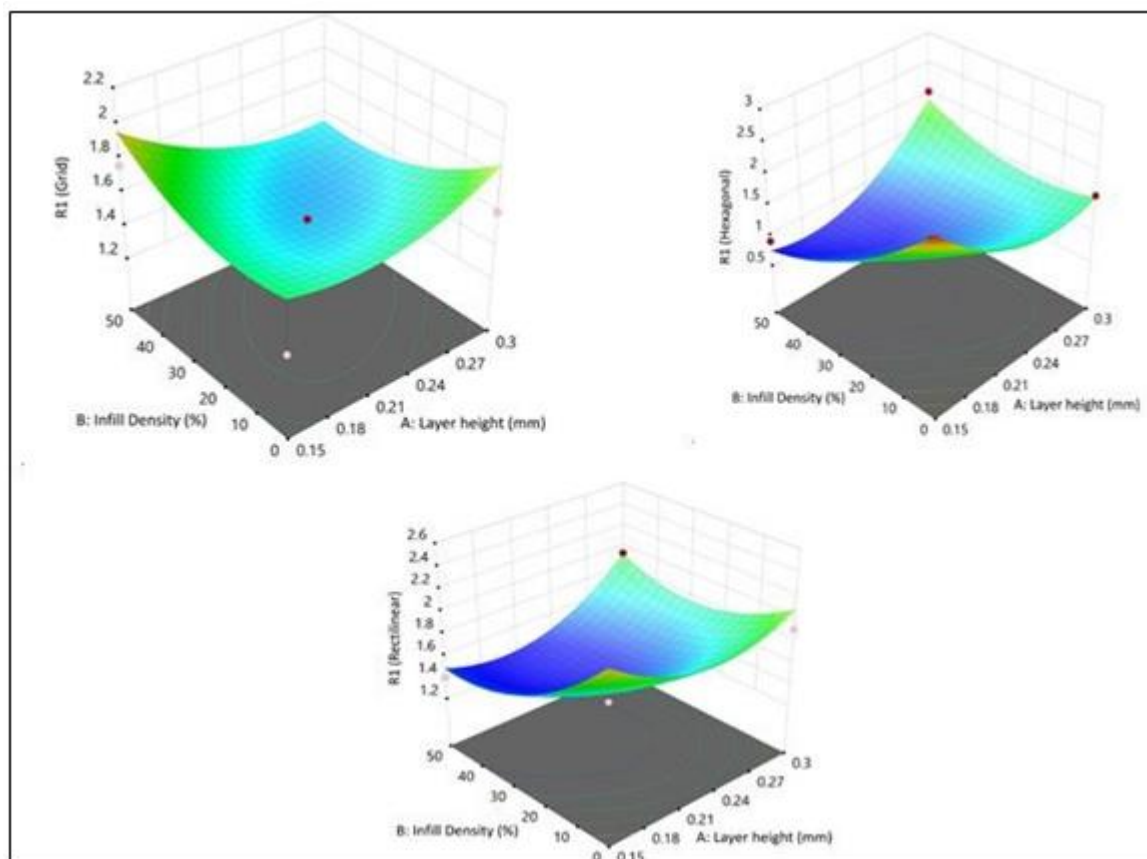


Figure 14. Surface graph prediction for flexural modulus of CF-ABS specimen

3.5. Impact energy of polymer and polymer composite

The impact energy represents its ability to absorb and disperse energies used to measure the strength of the material under shock loading. The Izod impact test was carried out on the impact tester according to the ASTM D256 standard. Samples were printed in an unnotched way, as the notching would cause rupture of deposited lines and a printed notched specimen would change the infill patterns. The impact energy of 3D printed polymer and polymer composite specimens are shown in Figures 15 and 16 respectively. Comparing the figures, the impact strength of CF-ABS composites is lower than ABS-printed specimens. The highest values are 5.3 Joule and 5 Joule in hexagonal printed pattern with 0.20 mm layer height and 50 % infill density for ABS and CF-ABS specimens respectively. From the graph, the impact strength of printed specimens increases with an increase in infill density. Increasing the infill density means a large amount of material is deposited into the printed part therefore the density of the part also increases. But as the layer height increases from 0.15 mm to 0.20 mm, their impact strength increases correspondingly [26]. The impact strength is higher in 0.20 mm printed layer thickness since the thickness of the layers will be more and hence these layers will act as a whole rather than providing adhesion. But an impact strength value varies for different infill patterns significantly. Among the groups for ABS and CF-ABS specimens grid patterns presented the lowest impact resistance and the highest impact strength is achieved in the hexagonal printed pattern. The lowest impact strength can be attributed to a simpler structure created by a grid pattern with no internal redundancies. Hence it is more susceptible to failure as cracks would create much higher strains in the internal structure. While the impact strength is almost similar in hexagonal and rectilinear patterns. The hexagonal and rectilinear patterns present higher symmetry which allows more energy absorption in the specimen. Even though the hexagonal pattern gives better impact strength it has internal angles and has higher mass too [18-20].

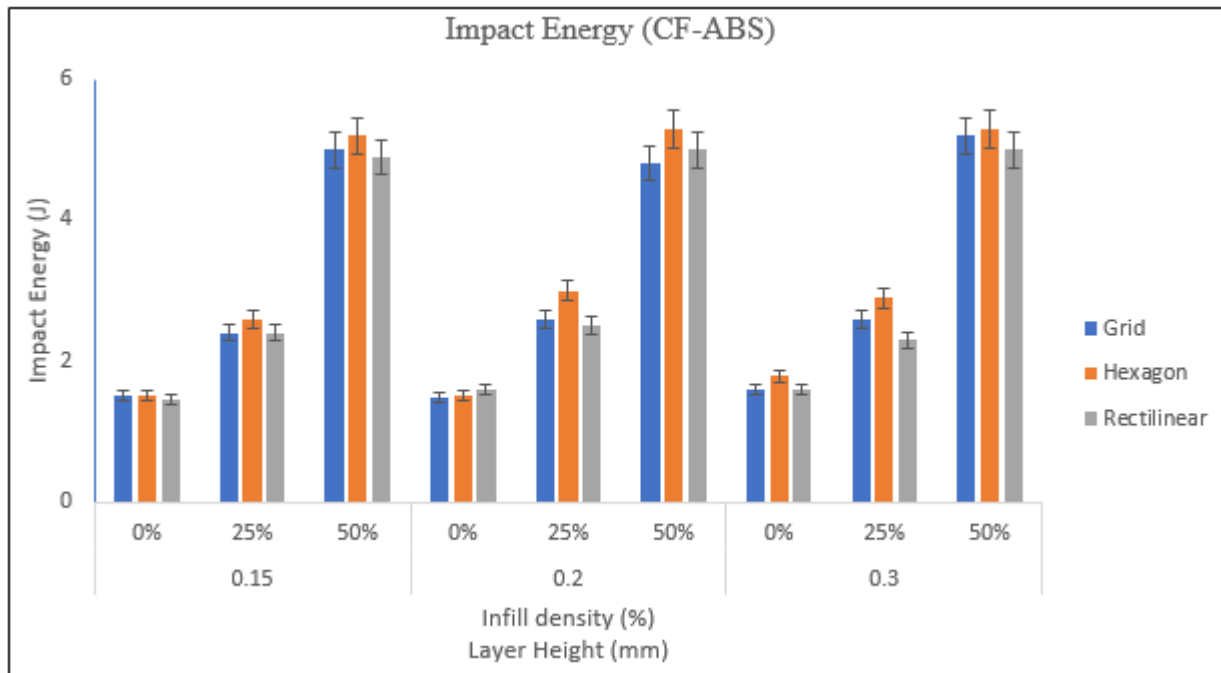


Figure 15. The impact energy of CF-ABS printed samples

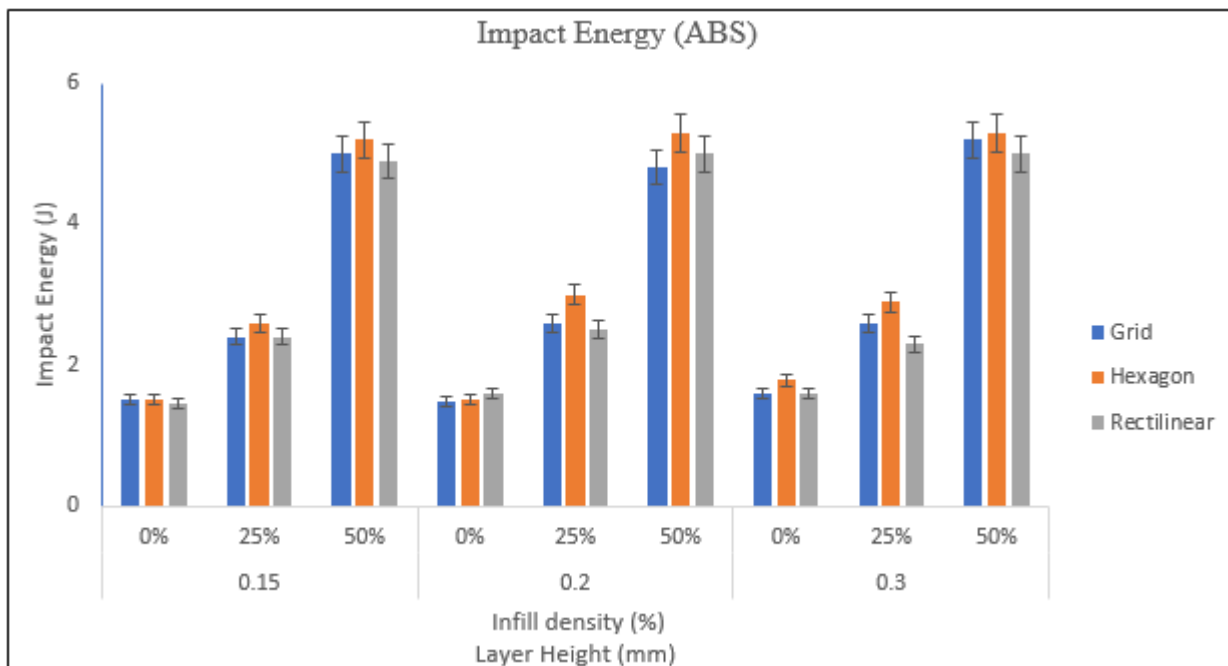


Figure 16. The impact energy of ABS printed samples

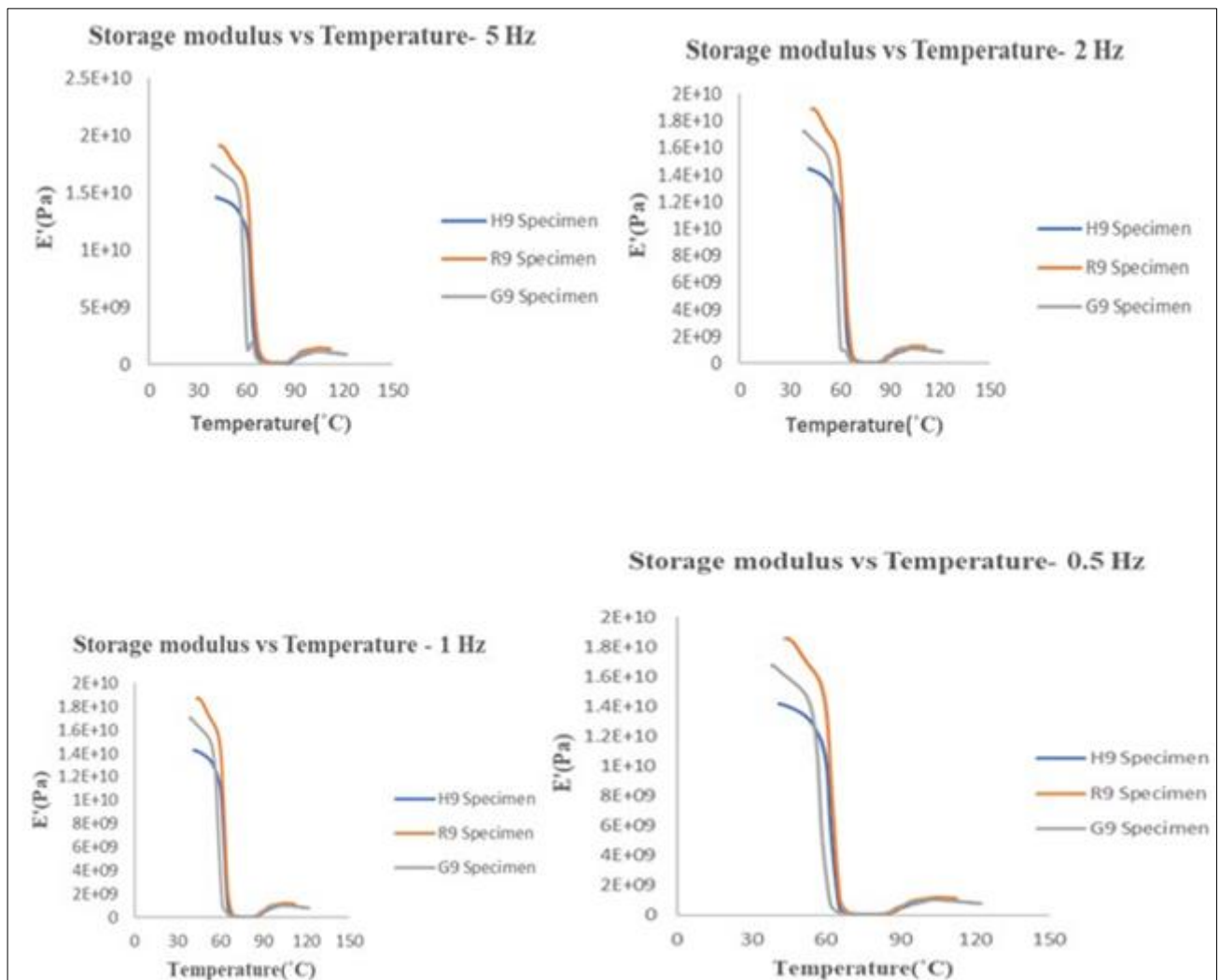
3.6. Dynamic mechanical analysis

It is a technique used to study the viscoelastic behavior of polymer and polymer composites. It helps to determine the storage modulus (E'), loss modulus (E''), loss factor ($\tan \delta$), and glass transition temperature (T_g) of polymer composite printed specimens under tensile mode. From the above results of mechanical properties, three specimens of CF-ABS material are printed using FFF for analysis of the viscoelastic behavior of the material. For those three specimens, a variation of 50% infill density, 0.30 mm layer thickness,

and infill pattern (Grid, Hexagon, and Rectilinear) is printed for investigation purposes. Finally, the effect of frequency on the above properties is presented with the help of a graphical chart.

3.6.1. Influence of temperature and frequency on the storage modulus

The Storage modulus measures the stiffness and elasticity of composite material and it indicates how much amount of energy is stored in the material during cyclic loading at varying temperatures [21]. As a function of temperature storage modulus is an essential parameter for DMA in analyzing mechanical properties. The effects of temperature on dynamic storage modulus for three different specimens at the frequency of 5, 2, 1, 0.5, and 0.2 Hz are shown in Figure 17. From the figure, it can be seen that all samples are in the glassy state below 50 °C and rubbery state above 60 °C. The glass transition region is from about 50 to 60 °C. The figure shows that E' decreases with increasing temperature and increases with increasing frequency. This is attributed to the lesser mobility of polymeric chains at high frequency. At higher frequency, the time available for movement of molecules is lesser which affects the localized stress concentration and this leads to increased stiffness of composite material. Also, it revealed that the storage modulus of hexagonal printed specimens is quite large in the glassy state while it changes slightly and remains the same in the rubbery state [22]. Hexagon printed pattern which contains crystalline structures shows a very gradual decrease after the onset of glass transition temperature when compared to the rectilinear and grid patterns.



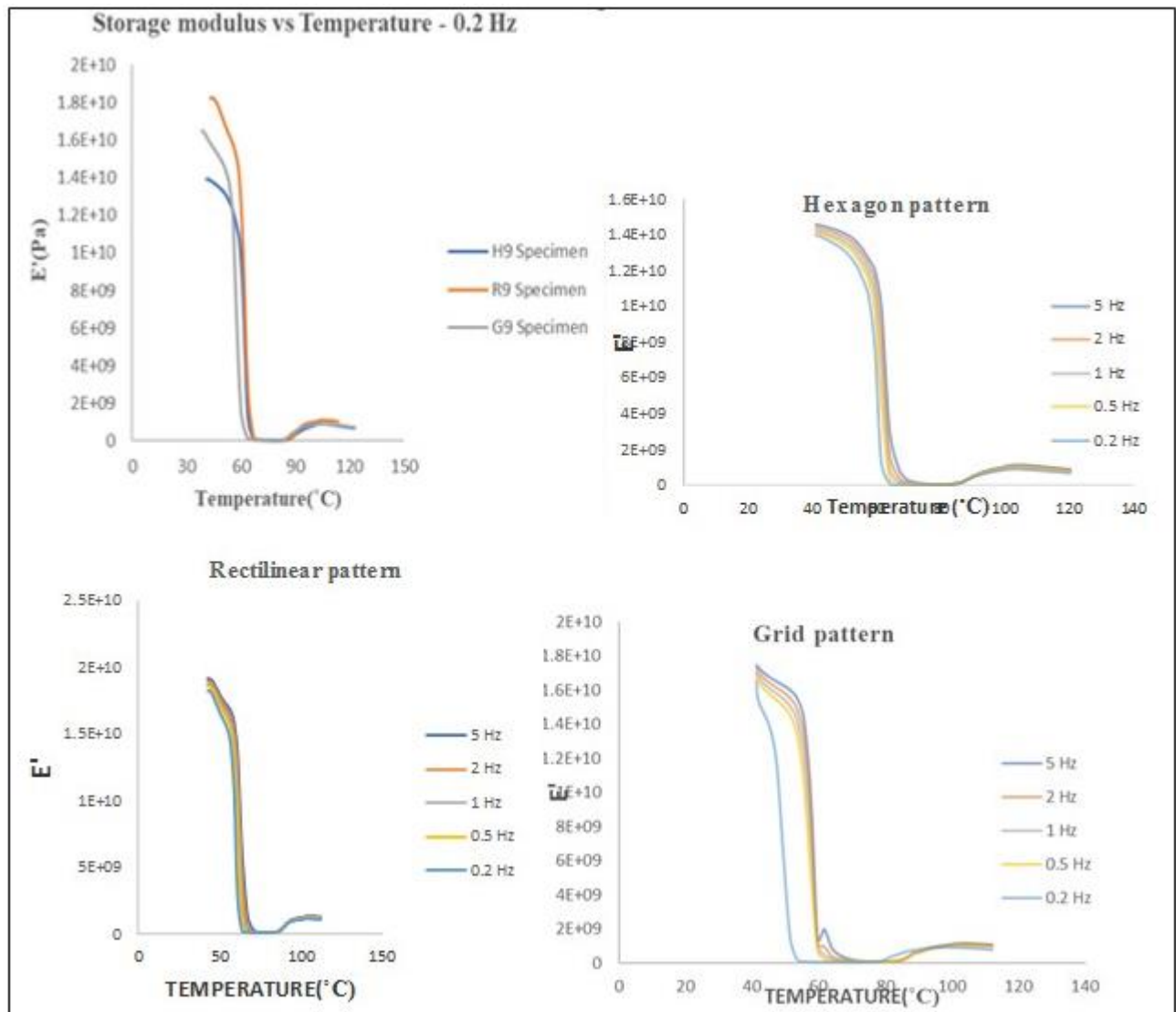
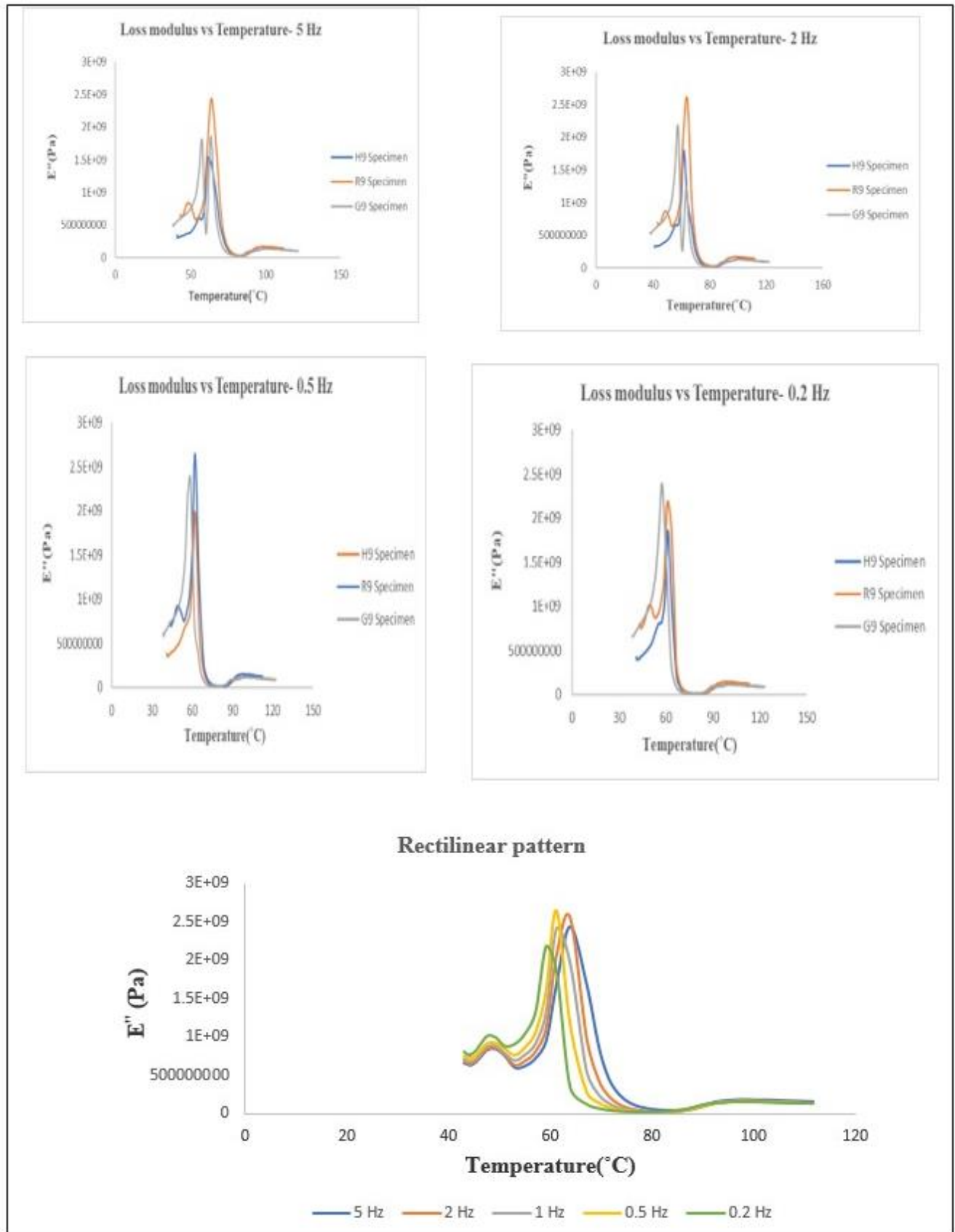


Figure 17. Influence of temperature and frequency on Storage modulus

3.6.2. Influence of temperature and frequency on loss modulus

The loss modulus represents the damping behavior which indicates the polymers' ability to disperse mechanical energy through intermolecular motions. Figure 18 shows the loss modulus of polymer composites for different infill patterns at varying frequencies as a function of temperature. The loss modulus is higher for the specimen printed with the rectilinear pattern at all frequencies. This is due to a less stiff structure which results in the dissipation of more energy. Therefore, loss modulus peaks are shifted towards higher temperatures which indicate higher thermal stability of the material. After the maximum peak, the loss modulus decreased due to the increase in polymer chain mobility [23, 24].



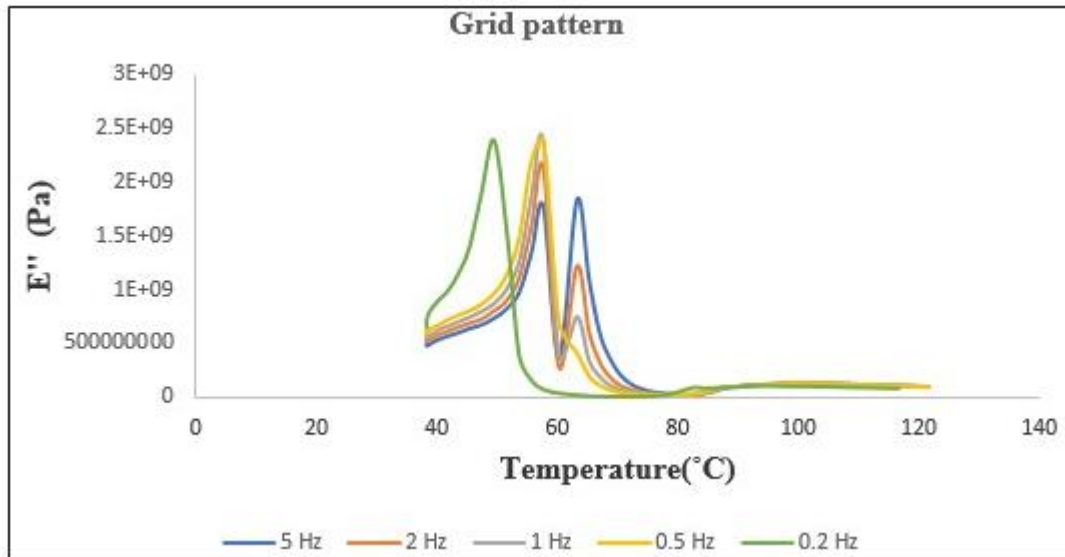
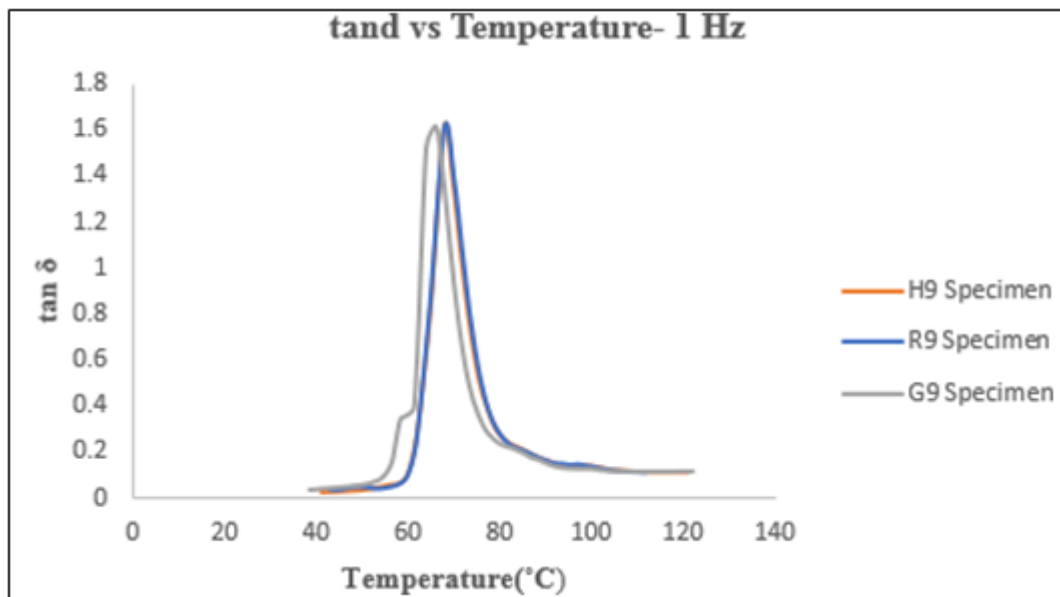
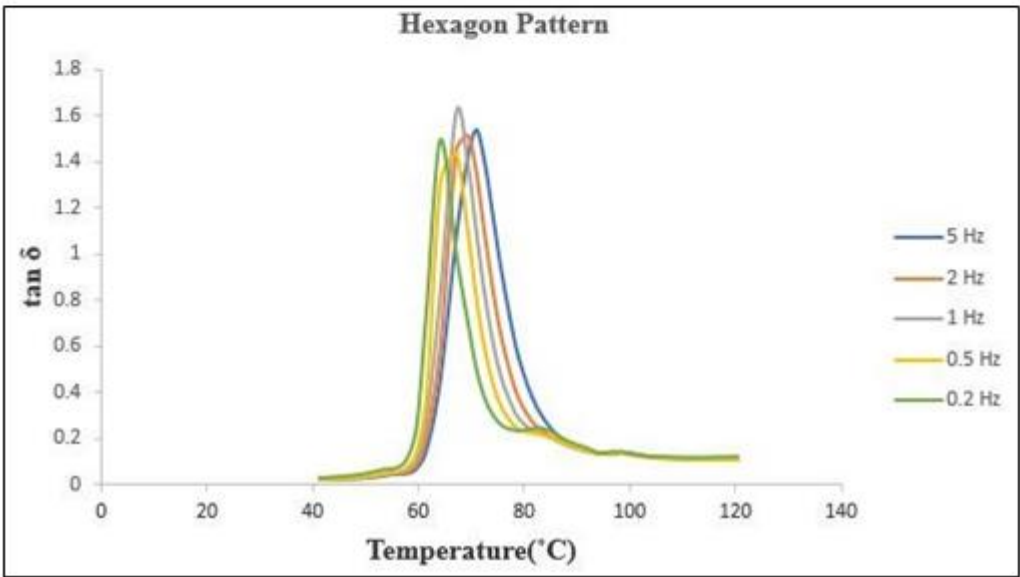
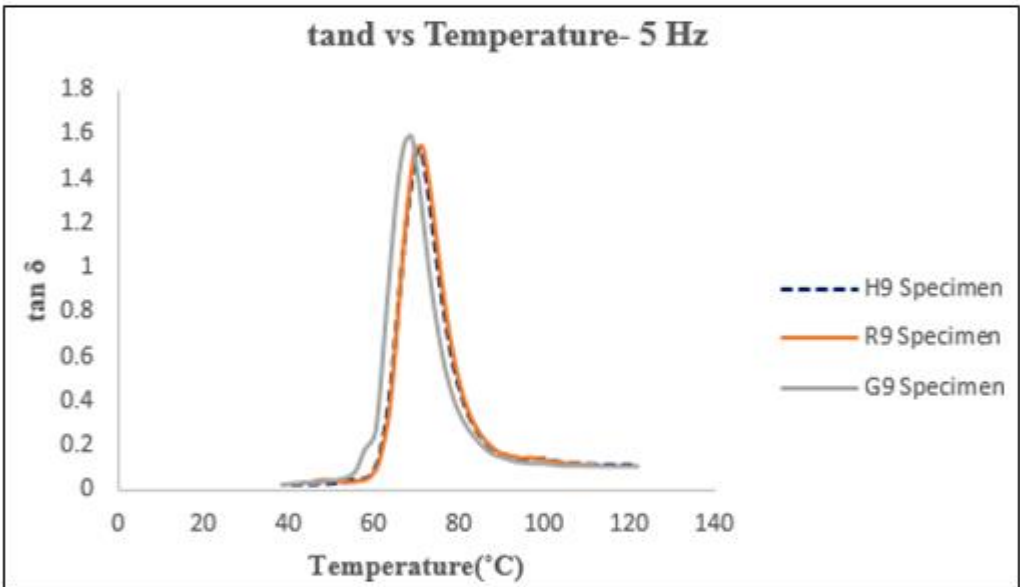
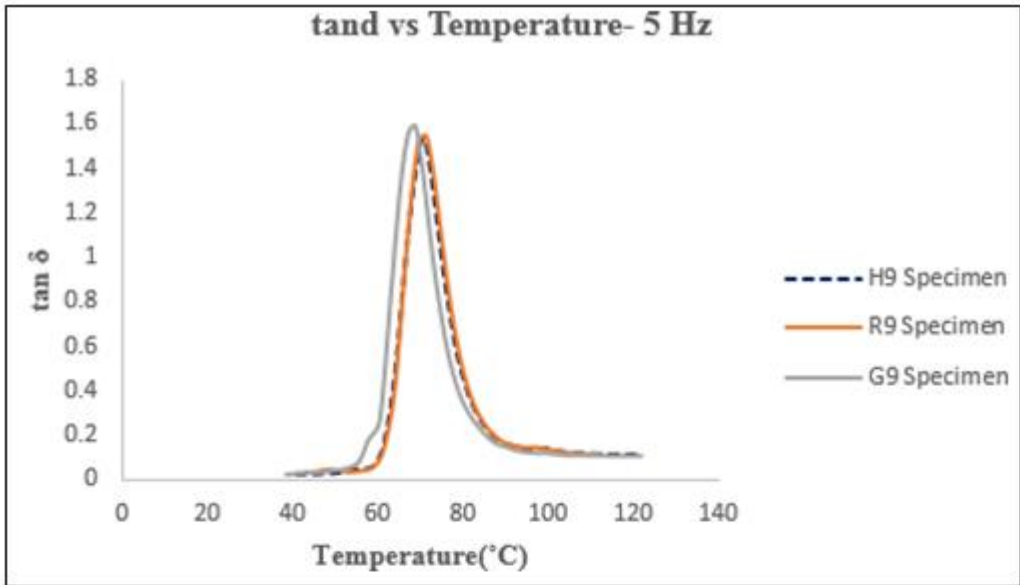


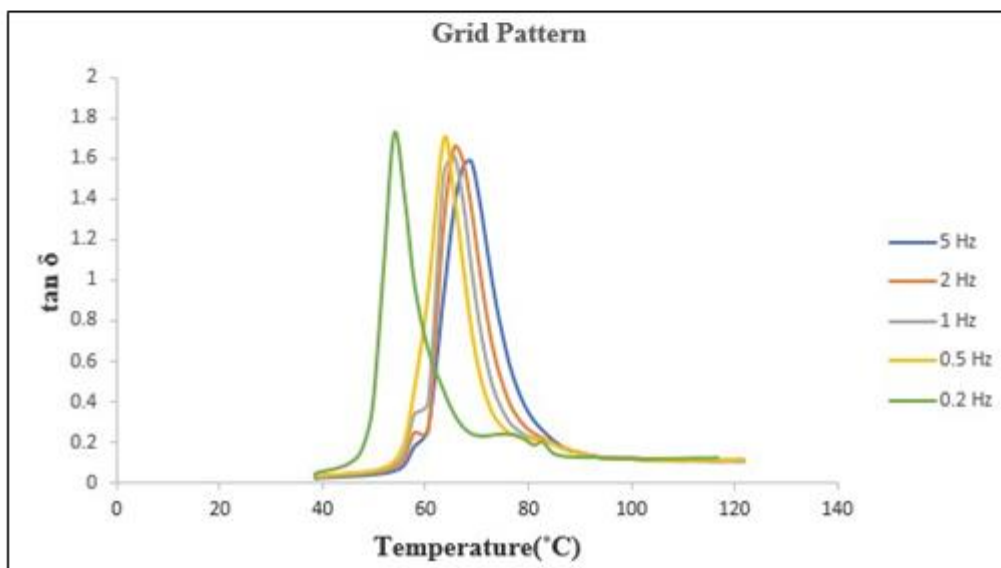
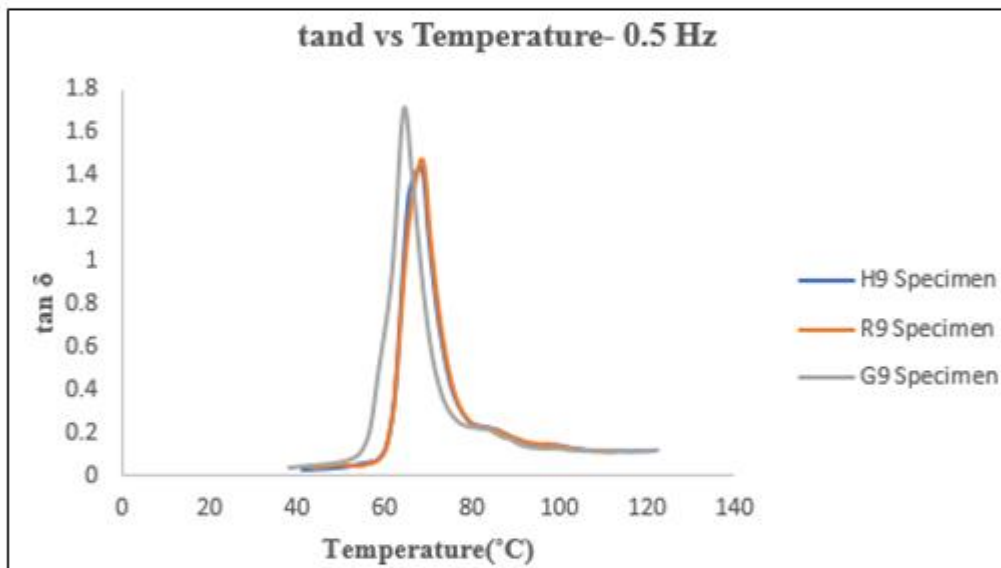
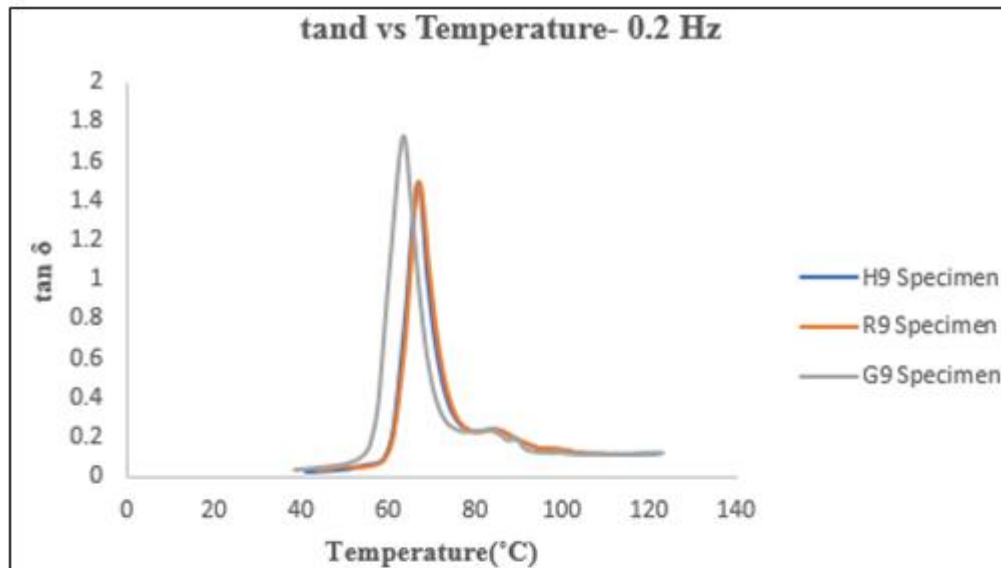
Figure 18. Influence of temperature and frequency on loss modulus

3.6.3. Influence of temperature and frequency on loss factor

The ratio of loss modulus to storage modulus is called the material loss factor. It helps us to determine the energy-absorbing behavior of materials. Figure 19 shows the $\tan \delta$ values for different infill patterns with varying frequencies as a function of temperature. Increasing the values of loss factor means the material has the potential for more energy dissipation whereas lower values mean the material has the potential to store load. It is observed from these figures that as the frequency increases from 0.5 Hz to 5 Hz the loss factor curves shifted that is the width of the $\tan \delta$ becomes wider. As mentioned earlier, the temperature corresponding to the loss factor peak is the T_g . Higher T_g values are seen from figures at higher frequencies. The loss factor is higher in hexagonal printed pattern with 50 % infill density, and 0.30 mm layer height for 1 Hz [25-30].







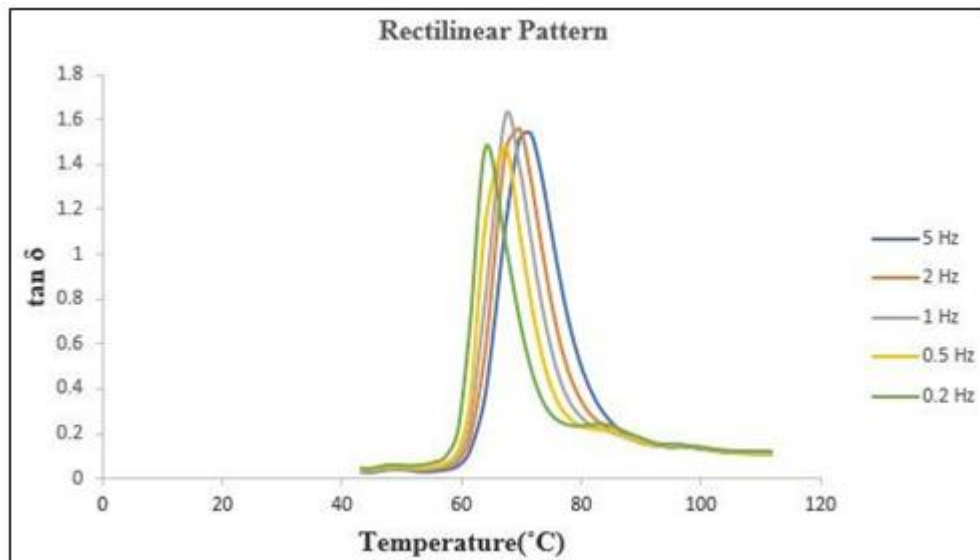


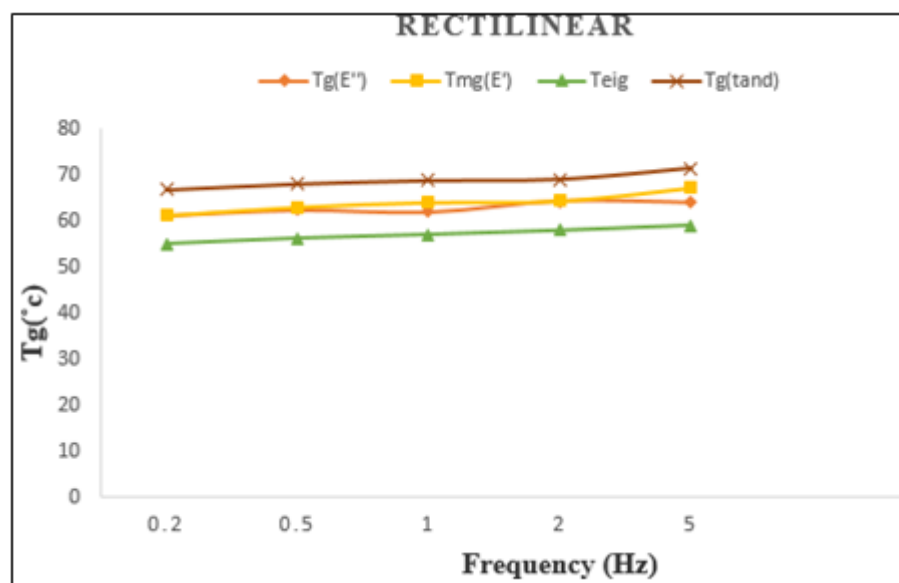
Figure 19. Influence of temperature and frequency on loss factor

3.6.4. Influence on frequency on glass transition temperature (T_g)

Figure 20 depicts the relationship between T_g and loading frequencies under tensile mode for hexagon, rectilinear, and grid patterns. It shows the changes in four kinds of T_g at different loading frequencies. With increasing frequency, the differences between $T_{g(E'')}$ and $T_{g(tan \delta)}$ become very larger. It means that the region of glass transition becomes wider when frequency increases. The graph shows that as the frequency increases the glass transition temperature is shifted to a higher temperature. The glass transition temperature may be expressed in the form of an Arrhenius-type equation (1) with frequency, which was widely used not only in DMA. This effect is attributed to different chain segments having different relaxation times. The relaxation time of small chain segments is short, and thus their T_g is lower than those of large chain segments. The glass transition region is related to the size distributions of chain segments. When the frequency increases, the T_g of both small and large chain segments increase. However, the increase in the T_g of the small chain segment is smaller than that of the large chain segment. This may cause the glass transition region to widen [31].

$$f = A \cdot \exp \left(- \frac{\Delta E}{R \cdot T_g} \right) \quad (1)$$

where ΔE is the Arrhenius activation energy, R is the gas constant and A is a constant.



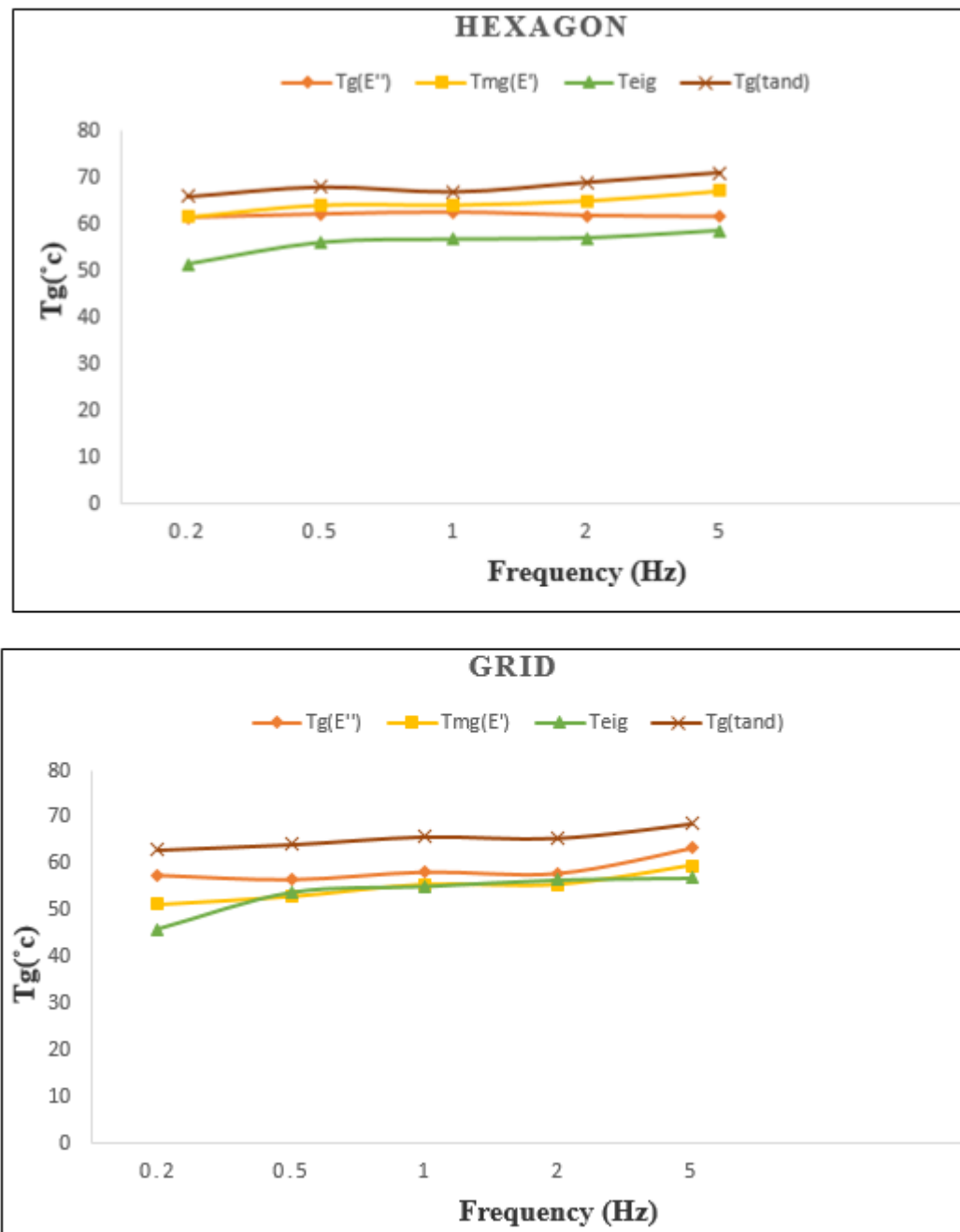


Figure 20. Influence of frequency on glass transition temperature

3.7. Micrographic characterization of polymer composite printed samples

Figures 21, 22, and 23 show the microscopic images of CF-ABS printed samples for hexagon, rectilinear, and grid patterns with the highest tensile properties. The tensile properties are highest in the hexagon pattern and lowest in the rectilinear and then grid patterns for ABS with and without CF reinforcement. Their tensile strength order is Hexagon > Rectilinear > Grid. From the microscopic image, it shows that in a hexagonal pattern, the specimen is filled with a large number of the hexagon in occupied space area compare to other patterns, also there bonding is very close to each other and each layer is deposited properly with previous layers and help us to withstand loads and transfer stress between layer to layers [32-35]. There are two different failures i.e., trans-raster failure and inter-raster failure in tensile testing of various printed samples. Generally, beads are deposited along the length of the specimen and are aligned in the direction parallel to the load applied during the tensile test. Therefore, beads are pulled parallel to the loading direction which results in a trans – raster failure. Finally, the individual beads withstood most of the applied load [17, 18].



Figure 21. Micrographic analysisiis of Hexagon Pattern (50% infill)

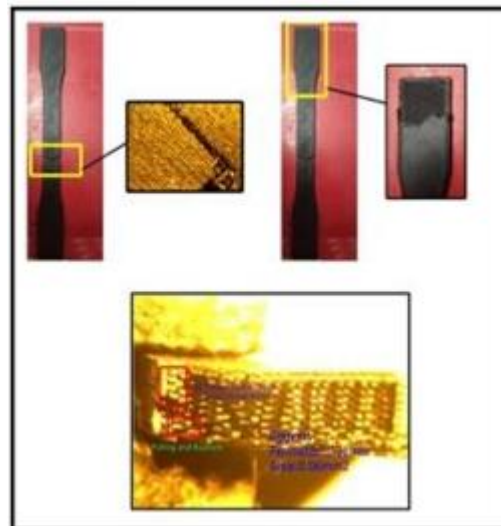


Figure 22. Micrographic analysisiis of Rectilinear Pattern (50% infill)

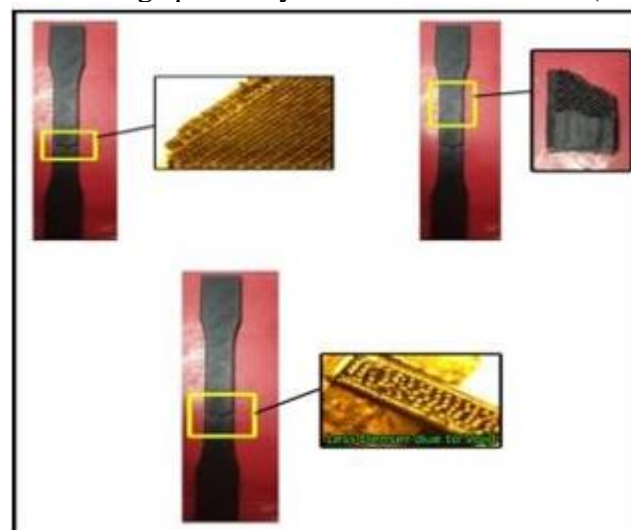


Figure 23. Micrographic analysisiis of Grid Pattern (50% infill)

So, the acting load yield high resistance to tensile failure and give maximum tensile strength which shown in Figure 22. Rectilinear and Grid pattern has almost equal strength but it is filled with fewer patterns for

occupied space area compare to the hexagonal pattern. Therefore, in low infill density patterns, their infill structure shape creates a high void during printing. The deposition trajectory and interlayer bonding were poor in this and micrographic images depict that their bonds with different layers are attached with a single point [36,37]. Similarly, when compared to the grid and rectilinear pattern, the grid pattern takes more printing time with the same infill density.

3.8. Scanning Electron Microscopy (SEM)

SEM images of the cross-section on the broken tensile and flexural CF-ABS specimens are shown in Figures 24 and 25. From the image, it is observed that 50% infill density with hexagonal pattern printed specimen gives better layer arrangement over the previous layer and the small air gap is present when compared to 50 % infill density with grid pattern printed samples [37-40]. This small air gap and high dense structure lead to a higher tensile and flexural property in the specimen.

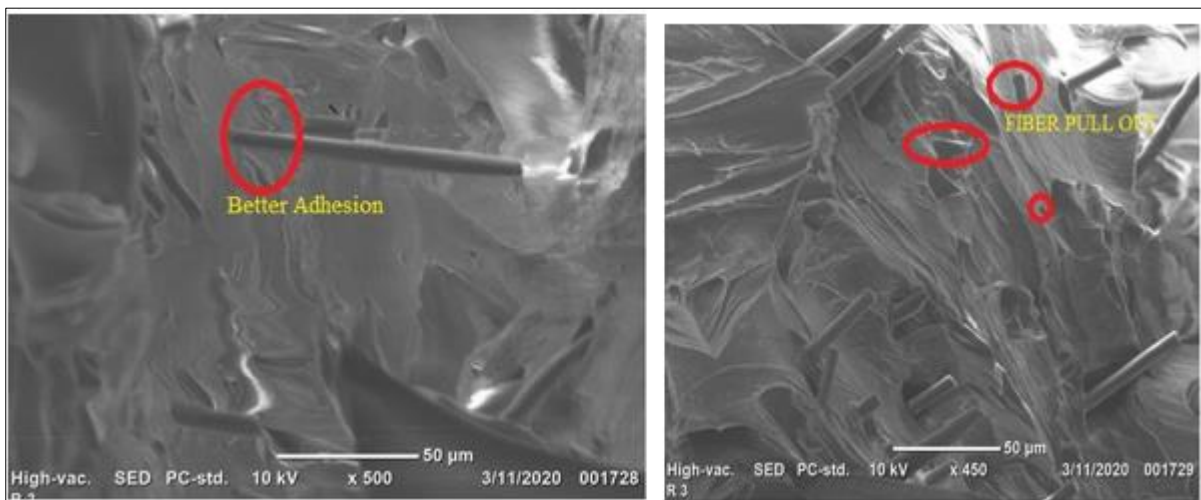


Figure 24. SEM image of Tensile fractured section

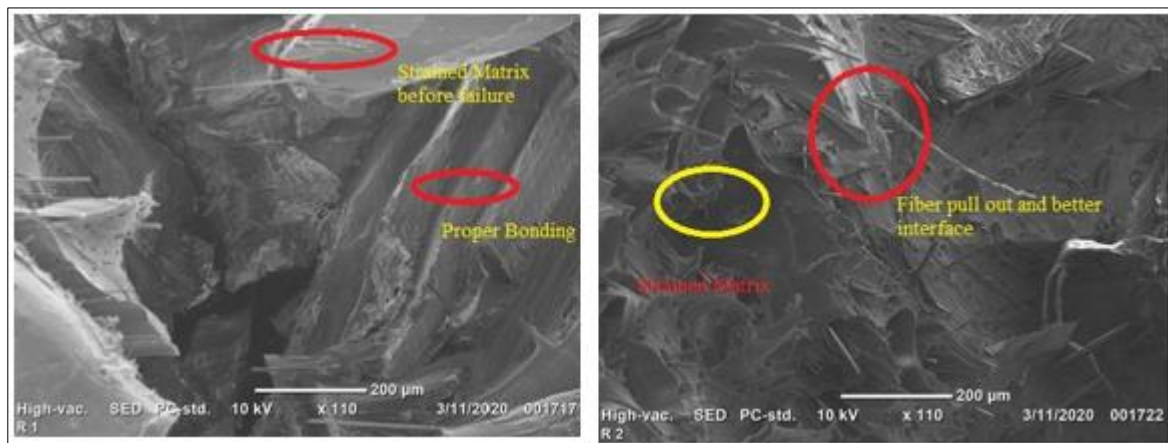


Figure 25. SEM image of Flexural fractured cross section

3.9. Fractography analysis of Fractured Specimens for CF-ABS

The fractured images are shown in Figure 26. Among images the Figure 26a, it visualizes a large number of voids present in the matrix fiber interfaces that lead to failure. Figure 26b shows that the improved mechanical strength was achieved due to adhesion between the carbon fiber and ABS matrix and it shows that the pattern even after the fiber failure, the matrix takes up a load and undergoes larger elongation before complete failure. Figure 26c shows that the main reason for the failure is due to improper fiber adhesion at the interface and resin breakage takes place [40-44].

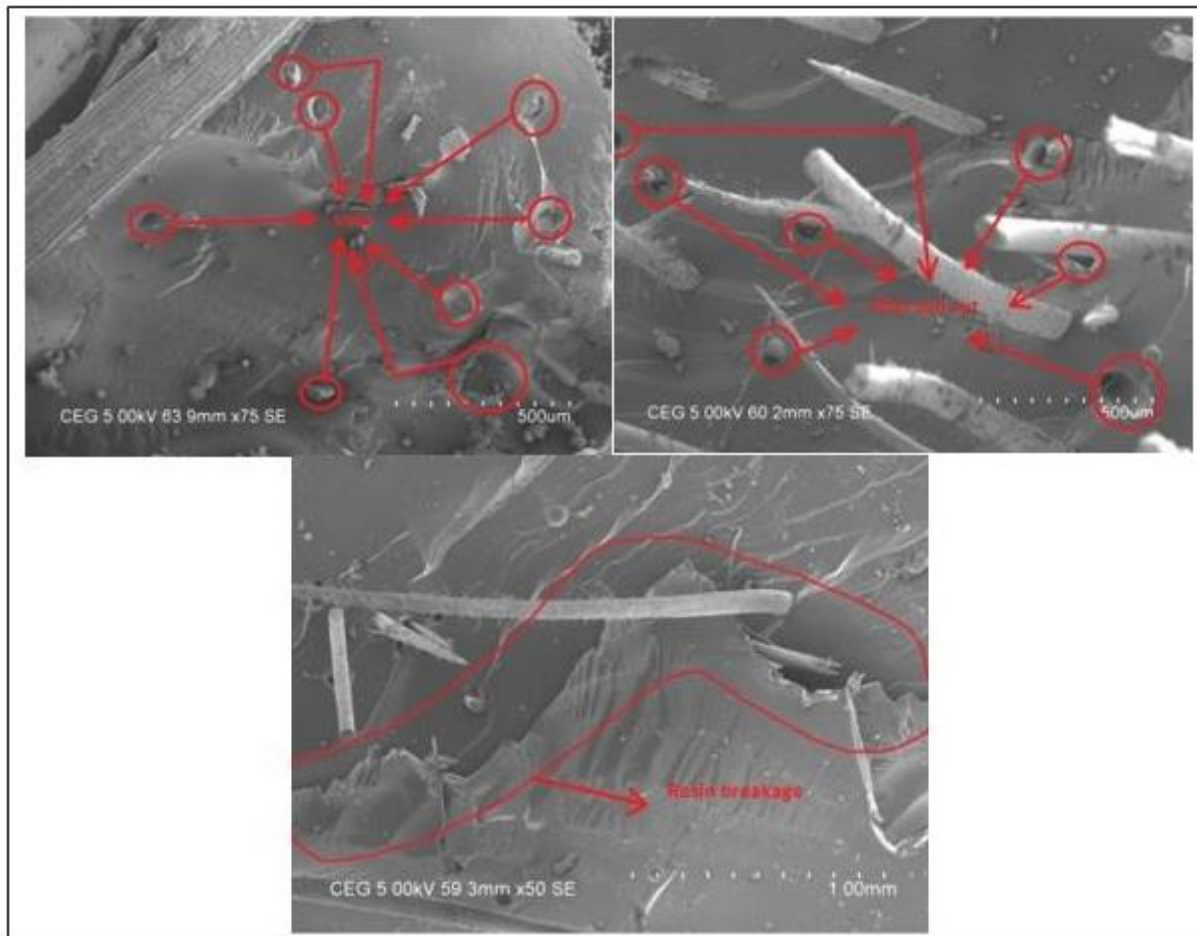


Figure 26. Fractography analysis

4. Conclusions

The following findings are obtained from current experimental research work to quantify the impacts of infill pattern, infill density, and layer thickness on static and dynamic mechanical properties of FFF printed ABS and CF-ABS specimens:

- as compared to all the patterns, specimens constructed with hexagonal patterns display a 25% improvement in mechanical properties (Tensile, Flexural, and Impact). The mechanical properties increase with infill density and exhibit maximum strength for the specimen built with 50% infill density, of the next significant observation. Finally, when compared to layer height, an increase in layer thickness increased mechanical properties by 0.15 mm to 0.20 mm. At lower layer heights, each layer was properly deposited on the previous layer, with no voids or air gaps;
- the DMA revealed that the hexagonal CF-ABS composite specimen has the highest storage modulus and glass transition temperature. It also revealed that at higher frequencies, molecular movement decreases, stabilizing the composite behavior and lowering the $\tan \delta$ value;

the reinforcement by carbon fiber in ABS has significantly improved the mechanical properties in static and dynamic tests, as well as the ability to withstand high temperatures. As a result, it is confirmed that CF-ABS material is a substantial and promising material for aerospace, automobile, and various industrial applications. Furthermore, research is needed to reduce void formation and improve interlayer bonding during the FFF process.

References

1. GOY, J.L., LADOS, D.A., ZHAI, Y., Additive Manufacturing: Making imagination the major limitation, *The Journal of Minerals and Material Society*, 66(5), 2014, 808–816
2. ABDULHAMEED, O., AL-AHMARI, A., AMEEN, W., MIAN, S. H., Additive manufacturing: Challenges, trends, and applications, *Advances in Mechanical Engineering*, 11(2), 2019
3. DILBEROGLU, U.M., DOLEN, M., GHAREHPAPAGH, B., YAMAN, U., The Role of Additive Manufacturing in the Era of Industry 4.0, *Procedia Manufacturing*, 11, 2017, 545–554
4. BALDASSARRE, F., RICCIARDI, F., The Additive Manufacturing in the Industry 4.0 Era: The Case of an Italian FabLab. *Journal of Emerging Trends in Marketing and Management*, 1(1), 2017, 105–115
5. DEHGHANGHADIKOLAEI, A., EMAMIAN, S.S., FOTOVVATI, B., GISARIO, A., MEHRPOUYA, M., VOSOOGHNI, A., The potential of additive manufacturing in the smart factory industrial 4.0: A Review, *Applied Sciences*, 9(18), 2019, 3865
6. DEY, A., YODO, N., A Systematic Survey of FDM Process Parameter Optimization and Their Influence on Part Characteristics, *Journal of Manufacturing and Materials Processing*, 23(3), 2019, p 64
7. CONEJERO, A., FERNANDEZ-VICENTE, M., FERRANDIZ S., Effect of Infill Parameters on Tensile Mechanical Behavior in Desktop 3D Printing, *3D Printing and Additive Manufacturing*, 3(3), 2016, p183–192
8. CONG, W., NING, F., QIU, J. WEI, WANG, S., Additive manufacturing of carbon fiber reinforced thermoplastic composites using fused deposition modeling, *Composites Part B: Engineering*, 80, 2015, 369–378
9. DAVE, H.K., PATADIYA, N.H., PRAJAPATI, A.R., RAJPUROHIT, S.R., Effect of infill pattern and infill density at varying part orientation on tensile properties of fused deposition modeling printed polylactic acid part, *Proceedings of the Institution of Mechanical Engineers Part C: Journal of Mechanical Engineering Science*, 235(10), 2019, 1811–1827
10. BOGREKCI, I., DEMIRCIOGLU, SUCUOGLU, H., TURHANLAR, O., The effect of the infill type and density on the hardness of 3d printed parts. *International Journal of 3D Printing Technologies and Digital Industry*, 3(3), 2019, p.212 – 219
11. JATTI, V.S., PATEL, A.P., A Study on Effect of Fused Deposition Modeling Process Parameters on Mechanical Properties, *International Journal of Scientific & Technology Research*, 8(11), 2019, 689–693
12. SHUBHAM, P., SIKIDAR, A., CHAND, T., The Influence of Layer Thickness on Mechanical Properties of the 3D Printed ABS polymer by Fused Deposition Modeling, *Key Engineering Materials*, 706, 2016, p 63–67
13. NUGROHO, A., ARDIANSYAH, R., RUSITA, LARASATI, I.L., Effect of layer thickness on flexural properties of PLA by 3D printing, *Journal of Physics: Conference Series*, 1130, 2018, 012017
14. KUMAR, M., RAMAKRISHNAN, R., OMARBEOVA, A., 3D printed polycarbonate reinforced acrylonitrile-butadiene-styrene composites: Composition effects on mechanical properties, micro-structure and void formation study, *Journal of Mechanical Science and Technology*, 33(11), 2019, 5219–5226
15. VIGNESHWARAN, K., VENKATESHWARAN, N., Statistical analysis of mechanical properties of wood-PLA composites prepared via additive manufacturing, *International Journal of Polymer Analysis and Characterization*, 24(7), 2019, 584–596
16. CHRISTIYAN, K.G.J., CHANDRASEKHAR, U., VENKATESWARLU, K., A study on the influence of process parameters on the Mechanical Properties of 3D printed ABS composite, *IOP Conference Series: Materials Science and Engineering*, 114, 2016, p.012109
17. WENZHEANG, W., GENG, P., ZHAN, P., ZHAO, J., Influence of Layer Thickness and Raster Angle on the Mechanical Properties of 3D-Printed PEEK and a Comparative Mechanical Study between PEEK and ABS, *Materials*, 8(9), 2015, 5834–5846
18. TEKINALP, H.L., VELEZ-GARCIA, G.M., DUTY, C.E., LOVE, I.J., NASKAR, A.K., BLUE, C.A., OZCAN, S., Highly oriented carbon fiber–polymer composites via additive manufacturing, *Composites Science and Technology*, 105, 2014, 144–150



19. ANDERSON, I., Mechanical Properties of Specimens 3D Printed with Virgin and Recycled Poly(lactic Acid), *3D Printing and Additive Manufacturing*, 24(2), 2017, 110-115
20. PAPON, EA., HAQUE, A., Tensile properties, void contents, dispersion and fracture behavior of 3D printed carbon nanofiber reinforced composites, *Journal of Reinforced Plastics and Composites*, 37(6), 2018, 381–395
21. AKHOUNDI, B., BEHRAVESH, AH., BAGHERI SAED, A., Improving mechanical properties of continuous fiber-reinforced thermoplastic composites produced by FDM 3D printer, *Journal of Reinforced Plastics and Composites*, 38(3), 2018, 99-116
22. ***ASTM D638-14. Standard test method for testing tensile properties of plastics
23. ***ASTM D790-15e2. Standard tests method for testing flexural properties of unreinforced and reinforced plastics and electrical insulating material
24. ***ASTM D256-10e1. Standard test method for determining Izod pendulum impact resistance of plastics
25. ABDULLAH, Z., TING, HY., HANDOKO, F., The effect of layer thickness and raster angles on tensile strength flexural strength for fused deposition modeling parts, *Journal of Advanced Manufacturing Technology*, 2017, 2289-8107
26. VEGA, V., CLEMENTS, J., LAM, T., The effect of layer orientation on the mechanical properties and microstructure of a polymer, *Journal of Material Engineering Performance*, 20(6), 2011, p 978-988
27. GARDAN, J., MAKKE, A., RECHO, N., A method to improve the fracture toughness using 3D printing by extrusion deposition, *Structural. Integrity Procedia*, 2016
28. J FENG, Z GUO, Effects of temperature and frequency on dynamic mechanical properties of glass/epoxy composites, *Journal of Materials Science*, 2016, 51, 2747-2758
29. IMALANATHAN, P., VENKATESHWARAN, N., SANTHANAM, V., Experimental investigation of mechanical and viscoelastic properties of Acacia Nilotica Filler Blende Polymer Composites, *Polymer Composites*, 2016, p24238
30. UMADEVI, I., BHAGAWAN, SS., Dynamic Mechanical Analysis of Pineapple Leaf/Glass Hybrid Fiber Reinforced Polyester Composites, *Polymer Composites*, 31, 2017, p. 956
31. CHENGDE, GU., WEI WHANG, LING REN, ZHENBIAO, Effects of magnesium on the microstructure and properties of Al-Si alloy deposited by wire and arc- based additive manufacturing, *Materials Technology*, 2020
32. NAVEED, Investigate the effect of process parameters on material properties and microstructural changes of 3D printed specimens using fusion deposition modeling, *Materials Technology*, 2020
33. ALIREZA MATBOUEI, AIREZA FATHI, SAYED MAHMOOD AND MASOUD SHIRZAD, Layered manufacturing of a three-dimensional polymethyl methacrylate (PMMA) scaffold used for bone regeneration, *Materials Technology*, 2018
34. ARIELLE MILLER, GRANT WARNER, GBADEBO OWOLABI, Mechanical Performance and Microstructural Analysis of Proton - Irradiated Fused Filament Fabrication Acrylonitrile Butadiene Styrene Material, *Journal of Material Engineering and Performance*, 2021, 30, p6673-6690
35. WILLIAM. H. FERRELL, JASON CLEMENT, STEPHAINE TER MAATH, Uniaxial tensile testing standardization for the qualification of fiber-reinforced plastics for fused filament fabrication, *Mechanics of Advanced Materials and Structures*, 2019
36. MATEUSZ GALEZA, ALEKSANDER HEJNA, PAULINA KOSMELA, ARKADIUSZ KULAWIK, Static and Dynamic Mechanical Properties of 3D Printed ABS as a Function of Raster Angle. *Materials*, 13(2), 2020, p297
37. ALINA RUXANDRA CARAMITU, RADU DASCALU, IOANA ION, VIOLETA TS AKIRIS, NICOLAE STANCU, MIHAELA ARADOAEI, ROMEO CRISTIAN CIOBANU, ADRIANA MARIANA BORS, IOSIF LINGVAY, Obtaining and Characterizing 3D Printable Polymer Based Composites with BaTiO₃ Filler, *Mater. Plast.*, **58**(1), 2021, 11-18
38. DAN IOAN STOIA, COSMINA VIGARU, CARMEN OPRIS, MARIUS VASILESCU, Properties and medical applications of biocompatible polyamide in additive manufacturing, *Mater. Plast.*, **58**(1), 2021, 113-120



39. YUAN ZHANG, YAN YIN, Investigation into the manufacturing process and properties of BrAl₁₀Fe₄ Aluminium-bronze parts by selective laser melting, *Materials Technology*, 2020, 35(13), 821-835
40. NAWAL ALHARBI, ALBERT J. VAN DE VEEN, DANIEL WISMEIJER, REHAM B. OSMAN, Build angle and its influence on the flexure strength of stereolithography printed hybrid resin material. An in vitro study and a fractographic analysis, *Materials Technology*, 34(1), 12-17
41. VINOTHBABU, N., VENKATESHWARAN, N., RAJINI, N., FARUQ MOHAMMED, HAMAD A.AL-LOHEAN, SUCHART SEINGCHIN, Influence of slicing parameters on surface quality and mechanical properties of 3D-printed CF/PLA composites fabricated by FDM technique, *Materials Technology*, 2020, 1-18
42. KHAN, SHAHROZ AKHTAR KUMAR, HARISH ARORA, PAWAN KUMAR, Retrospective Investigation on emergence and development of additive manufacturing, *Indian Journal of Engineering and Material Science*, 28(2), 2021
43. DAKOTA R HETRICK, SEYED HAMID REZA SANEI, OMAR ASHOUR, CHARLES E BAKIS, Charpy impact energy absorption of 3D printed continuous Kevlar reinforced composites, *Journal of Composite Materials*, 55(12), 2021, 1705-1713
44. JIURU, LU., LUYAO, XU., JUN HU, Micromechanical analysis of the tensile deformation behavior for 3D printed unidirectional continuous fiber reinforced thermos-plastic composites. *Journal of Mechanical Science and Technology*, 34, 2020, 5085-5092

Manuscript received: 29.09.2021